Response time analysis of a live-cube compact storage system with two storage classes

Nima Zaerpour, Yugang Yu & René B. M. de Koster

View supplementary material 🔗

Accepted author version posted online: 04 Jan 2017.
Published online: 04 Jan 2017.

Submit your article to this journal 🔗

Article views: 288

View related articles 🔗

View Crossmark data 🔗

Taylor & Francis
Taylor & Francis Group

🔓 OPEN ACCESS

Response time analysis of a live-cube compact storage system with two storage classes

Nima Zaerpour[a], Yugang Yu[b] and René B. M. de Koster[c]

[a]College of Business Administration, California State University San Marcos, San Marcos, CA, USA; [b]School of Management, University of Science and Technology of China, Hefei, P. R. China; [c]Rotterdam School of Management, Erasmus University, Rotterdam, The Netherlands

ABSTRACT

We study a next generation of storage systems: live-cube compact storage systems. These systems are becoming increasingly popular, due to their small physical and environmental footprint paired with a large storage space. At each level of a live-cube system, multiple shuttles take care of the movement of unit loads in the x and y directions. When multiple empty locations are available, the shuttles can cooperate to create a virtual aisle for the retrieval of a desired unit load. A lift takes care of the movement across different levels in the z-direction. Two-class-based storage, in which high turnover unit loads are stored at storage locations closer to the Input/Output point, can result in a short response time. We study two-class-based storage for a live-cube system and derive closed-form formulas for the expected retrieval time. Although the system needs to be decomposed into several cases and sub-cases, we eventually obtain simple-to-use closed-form formulas to evaluate the performance of systems with any configuration and first zone boundary. Continuous-space closed-form formulas are shown to be very close to the results obtained for discrete-space live-cube systems. The numerical results show that two-class-based storage can reduce the average response time of a live-cube system by up to 55% compared with random storage for the instances tested.

1. Introduction

Live-cube compact storage systems have recently been introduced in automated storage systems. They can achieve a high storage density together with short response times with unit loads being individually able to move in a three-dimensional space. They have many applications, including parking systems, warehouses, and container terminals (Hyundai Elevator, 2012; Magic Black Box, 2012; Park, Swipe, Leave Parking Systems, 2012; Space Parking Optimization Technology, 2012; UCW Container Storage Systems, 2012; Wohr Parksafe, 2012).

Such storage systems operate with electrically powered shuttles and lifts, which lead to significantly reduced fossil fuel and energy consumption and CO_2 emissions (Zaerpour *et al.*, 2017). Such systems have two features in common:

1. They are compact. Compact systems are aisle-less, reducing storage space and the environmental footprint compared with traditional storage systems (two-dimensional systems), which require drive aisles.
2. They have "live" storage. A live-cube compact storage system contains multiple levels of storage grids, shuttles, a lift, and a depot or an Input/Output (I/O) point. Shuttles can move in the x and y directions (provided that there is an empty space) while carrying a unit load. In a storage grid, each location can accommodate one shuttle and each unit load is stored on its own shuttle.

The pattern of shuttle movements has been compared to solving a Sam Loyd's 15-puzzle game (Slocum and Sonneveld, 2006). To maneuver a desired unit load to the lift at the unit load's storage level, shuttles have to move multiple unit loads aside into open locations, which have to be created first. Then, the lift takes care of movements across different levels in the z-direction (see Figure 1). We assume that the I/O point is located at the lower-left corner of the system. The lift waits at the I/O point when idle.

Compared with other types of compact storage systems (e.g., satellite-based systems or conveyor-based systems), a live-cube system has the major advantage of independent movements in three-dimensional space. The lift moves independently of the shuttles, shuttles at different levels move independently, and two shuttles can move independently of each other even at the same level.

The performance of a compact storage system in service sectors is often measured in terms of its response time. It has been shown in the literature that two-class-based storage can reduce the average response time of a storage system by up to 50% compared with random storage (Hausman *et al.*, 1976; Eynan and Rosenblatt, 1994; Kouvelis and Papanicolaou, 1995; Ruben and Jacobs, 1999; Park, 2006; Yu and de Koster, 2009). Two-class-based storage can be simply implemented in

Figure 1. A live-cube compact storage system.

practice by classifying unit loads into high turnover and low turnover classes. The high turnover unit loads are assigned to locations closer to the I/O point, resulting in shorter response times, due to the majority of customer requests being retrieved from locations closer to the I/O point. The performance of two-class-based storage highly depends on the storage system configuration, first zone boundary, and product turnover.

In this article, we study the performance of a two-class-based storage policy in a live-cube compact storage system. We derive closed-form formulas for the expected retrieval time of an arbitrary unit load for a two-class-based live-cube system with any rectangular system configuration, first zone boundary, and ABC curve. To obtain closed-form formulas, the system needs to be decomposed into several cases and sub-cases. Although the decomposition procedure is complicated, it can be split into 36 complementary cases, each corresponding to a unique closed-form formula for the expected retrieval time. Each case represents a specific system configuration and a first zone boundary range. The closed-form formulas can be used to instantaneously evaluate the performance of a two-class-based live-cube system. In addition, we investigate the impact of different sizes of the first zone for a fixed system configuration and compare the performance of systems with different configurations. We compare the closed-form formulas (which are based on a continuous space approximation) with the average response time of a discrete-space live-cube system in a real-life setting. The differences between the results of closed-form formulas and the ones obtained based on a discrete system are all less than 4%. In addition, we compare the performance of our proposed two-class-based storage policy with both random storage and cuboid-shaped two-class-based storage with a cuboid-shaped first zone. The results show that our two-class-based storage policy can significantly reduce the average response time of a live-cube system compared with random storage (up to 55%) and two-class-based storage with a cuboid-shaped first zone (up to 22%). The implementation of such a two-class-based storage policy requires no modification of the system configuration and no additional investment in infrastructure.

Automated material handling systems have been extensively studied in the literature. For a general review on the design and control of automated material handling systems, we refer to Johnson and Brandeau (1996) and Roodbergen and Vis (2009). A particular area of study involves travel time models. Hausman *et al.* (1976) were the first to study travel time models for an Automated Storage and Retrieval (AS/R) system. They propose

closed-form expressions for the travel time in a Square-In-Time (SIT) continuous rack under different storage policies. Graves *et al.* (1977) extend that work by considering interleaving times in their travel time model. Bozer and White (1984) develop closed-form expressions for the expected travel time for a non-SIT rack and random storage. Based on simulation results, they show that the model is quite accurate. Since then, researchers have continued studies in the same direction, such as derivation of closed-form expressions for travel time (Kim and Seidmann, 1990; Sarker *et al.*, 1991) and system optimization based on closed-from expressions obtained in previous studies (Rosenblatt and Eynan, 1989; Eynan and Rosenblatt, 1994; Kouvelis and Papanicolaou, 1995). In addition, several authors studied models of the travel time for other types of storage and retrieval systems. These systems include multi-shuttle AS/R systems (Sarker *et al.*, 1991; Keserla and Peters, 1994; Malmborg, 2000), miniload AS/R system (Park *et al.*, 2003; Park, 2006), and compact storage systems (De Koster *et al.*, 2008; Yu and de Koster, 2009; Zaerpour *et al.*, 2015).

The literature on compact storage systems is quite small. Based on system type, papers can be divided into five groups. Stadtler (1996) and Zaerpour *et al.* (2015) study (1) *deep-lane compact storage systems with satellites* from an operational decision-making level, aiming at shorter response times. Stadtler (1996) proposes a storage and retrieval assignment algorithm. Zaerpour *et al.* (2015) propose a shared storage assignment policy for such a system, in order to minimize total retrieval time of customer requests while avoiding reshuffling. Malmborg (2002), Fukunari and Malmborg (2007), Kuo *et al.* (2007), and Roy *et al.* (2015) study (2) *Autonomous Vehicle Storage and Retrieval* (AVS/R) systems for various storage and dwell point policies. Within the storage rack, the key distinction of AVS/R systems is the movement patterns of the handling system. In an AVS/R system, vehicles share a fixed number of lifts for vertical movements and follow rectilinear paths in two dimensions for horizontal movements. Sari *et al.* (2005), De Koster *et al.* (2008), and Yu and de Koster (2009) study (3) *conveyor-based compact storage systems*. In these systems, rotating conveyors move unit loads in the deep storage lanes. To access a unit load, other unit loads also need to be moved by the rotating conveyor. Sari *et al.* (2005) study a system where a lift takes care of the vertical movement of unit loads. They obtain closed-form formulas for the travel time of loads for any system design. De Koster *et al.* (2008) and Yu and de Koster (2009) study the optimal design of systems where a crane moves unit

Table 1. Overview of types of compact storage systems.

Type	Transport system in length direction	Transport system in width direction	Transport system in height direction	Travel time function for retrieval from location (x, y, z)	References
Satellite-based system	S/R machine	Satellite	S/R machine	$2(\max\{x, y\}+z)$	Stadtler (1996); Zaerpour et al. (2015b)
AVS/R system	Autonomous vehicle	Autonomous vehicle	Lift	Dependent on the location of vehicles	Malmborg (2002); Kuo et al. (2007); Fukunari and Malmborg (2007); Roy et al. (2015)
Conveyor-based system	S/R machine	Power or gravity conveyor	S/R machine	$\max\{\max\{x, y\},z\}+\max\{x, y\}$	Sari et al. (2005); Yu and de Koster (2009); De Koster et al. (2008)
Puzzle-based system	Shuttle	Shuttle	—	$4\max\{x, y\}+2\min\{x, y\}$	Gue and Kim (2007)
Live-cube system	Shuttle	Shuttle	Lift	$\max\{x+y, z\}+z$ (if multiple empty locations are available per level)	Zaerpour et al. (2015a); This article

loads in horizontal and vertical directions. They optimally solve the retrieval time minimization problem by decomposing it into three cases. Gue and Kim (2007) study a (4) *single-level live-cube* system or a so-called puzzle-based system. They investigate the travel time (expressed in number of movements) of any unit load to the I/O point. Each load is stored on an individual shuttle. They derive closed-form formulas for a single-level system with one empty location and also develop a method to maneuver unit loads to the I/O point, minimizing the retrieval time of an arbitrary unit load. In addition, they propose a heuristic retrieval method that yields short retrieval times for systems with multiple empty locations. Mirzaei *et al.* (2017) extend Gue and Kim's paper by studying a multiple load retrieval problem in a puzzle-based storage system. They develop an optimal method for this problem by using a joint load retrieval location. Their results show that the total retrieval time can be significantly reduced by using the joint retrieval method. Zaerpour *et al.* (2017) study travel time in a (5) *multi-level live-cube compact storage system* considering a random storage policy. Through a decomposition procedure, they derive four closed-form travel time formulas corresponding to four complementary system configurations. Table 1 summarizes the types of compact storage systems, based on transport handling components and a travel time function, and gives the relevant references discussed above.

This article also studies travel time in multi-level live-cube systems. However, we focus on two-class-based storage. Applying a storage zone boundary significantly increases the complexity of the problem, leading to 36 cases that have to be distinguished in the decomposition process compared with four cases for the random storage problem. The remainder of this article is organized as follows. Section 2 describes the problem and assumptions. Section 3 derives the closed-form formulas for expected retrieval times of the first and second zones of a rectangular live-cube system. Section 4 describes our results, evaluates the quality of the closed-form formulas obtained based on the continuity assumption for a real-life discrete live-cube compact storage system, and compares the performance of two-class-based storage with random storage. We conclude and suggest avenues for future research in Section 5.

2. Problem description and assumptions

In this section, we first describe the two-class-based storage policy, the main assumptions (assumptions A1 , ..., A6), and the

general procedure to derive the expected retrieval time. Then we explain the mechanism of a live-cube storage system under a two-class-based storage policy.

A1: *The system and storage coordinates are assumed to be continuous.*

This assumption is commonly used in the literature (see Hausman *et al.* (1976), Bozer and White (1984), Rosenblatt and Eynan (1989), Yu and de Koster (2009)) and significantly reduces the complexity of the analysis.

A2: *The product and unit load turnover distribution can be derived from the Pareto-demand curve* (*ABC curve*) *and by assuming an Economic Order Quantity* (*EOQ*) *product replenishment model.*

The ABC curve represents the percentage of cumulative demand in number of unit loads versus the fraction of ranked inventoried products. Equation (1) gives a representation of the ABC curve function where p is the percentage of inventoried products (ranked in descending order based on their demand), and s is the skewness parameter. A smaller s means a more skewed curve (see Hausman *et al.* (1976)):

$$A(p) = p^s, \quad 0 < s \le 1, \tag{1}$$

where $\lambda(j)$ represents the turnover of the product on unit load j (j is normalized to be between zero and one) or, briefly, the turnover of unit load j in the system. Based on Hausman *et al.* (1976), using the EOQ policy, we find that

$$\lambda(j) = (2s/K)^{0.5} j^{\frac{s-1}{s+1}}, \quad 0 < j \le 1, \tag{2}$$

where K is the ratio of order cost to holding cost, which is assumed to be identical for all items. The expected retrieval time of a two-class-based system can be expressed as follows:

$$E[T] = \frac{\int_{j\in R_1} \lambda(j)E[T^1]dj + \int_{j\in R_2} \lambda(j)E[T^2]dj}{\int_{j=0}^{1} \lambda(j)dj}, \tag{3}$$

where $j \in R_i$ represents the unit loads assigned to locations in zone (region) i ($i = 1, 2$) and $E[T^i]$ is the expected retrieval time of a unit load in zone i. Let B represent the boundary of the first zone, which is the set of all locations with travel time distance b to the I/O point. Therefore, all locations with travel time distance less than or equal to the boundary parameter b form the first zone and the remaining locations of the system form the

(a) Retrieval request

Notes. (1) Requested unit load is in a different color

(2) Bold line represents first zone boundary

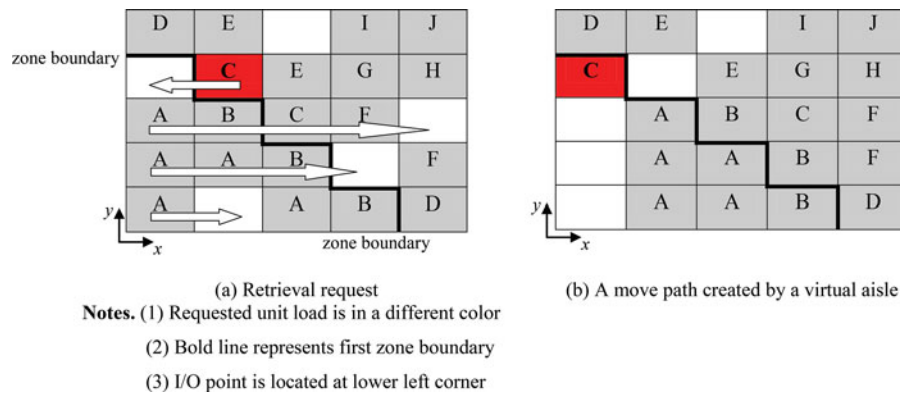(3) I/O point is located at lower left corner

Figure 2. A virtual aisle in a single-level live-cube system.

second zone. In Equation (3), $\lambda(j)$ can be replaced by the expression given in Equation (2). Since $2s/K$ is a constant that appears in both the numerator and denominator, it can be removed from the expression. The remaining part can be written as follows:

$$E[T] = G_1^{2s/(s+1)}E[T^1] + (1 - G_1^{2s/(s+1)})E[T^2], \qquad (4)$$

where G_1 is the volume of the first zone divided by the volume of the system (V^1/V).

Measured in the time dimension, a system has the following dimensions:

- a length l (the shuttle's travel time from/to the I/O point to/from the farthest location in the x-direction in an empty lane);
- a width or depth w (the shuttle's travel time from/to the I/O point to/from the farthest location in the y-direction in an empty lane);
- a height h (the lift's travel time from/to the I/O point to/from the farthest level in the z-direction).

A3: *For the sake of convenience and without loss of generality, we suppose that the length of the system is not less than the width of the system in time units; i.e., $l \geq w$ (see also Bozer and White (1984), Eynan and Rosenblatt (1994), and Yu and de Koster (2009)).*

The system storage capacity (lwh) is a constant. The travel time of a unit load to the lift location at a given level depends on its (x, y) position, and the distribution of empty locations on its path to the lift. In the case where only one empty location is available, Gue and Kim (2007) show that it is equal to $4x + 2y - 8$ (if $x > y$). However, in practice, the storage capacity of live-cube systems is not fully utilized. This implies that live-cube systems can be designed such that there are sufficient empty locations at each level to create a virtual aisle for any desired unit load.

A4: *We assume there are sufficient empty locations on each level to create a virtual aisle for a requested unit load.*

By creating a virtual aisle, the requested unit load can move to the lift location without interfering with other unit loads. A sufficient condition to create such a virtual aisle is that the number of empty locations on a level equals at least the maximum of the number of rows and the number of columns. For more details about the properties of such a system, we refer to Zaerpour *et al.* (2017). Figure 2(a) shows a situation where a unit load (product C) needs to be moved out of a live-cube system. In Figure 2(b) the virtual aisle is created by "block movement" of multiple unit loads simultaneously, which is possible if the retrieval path is a

straight line. While the vertical virtual aisle is being created, the load C can move in the horizontal direction leftward, thereby avoiding a constant time to create the virtual aisle. However, in a worst-case scenario, a small constant time is required to create a virtual aisle (maximum time to create a virtual aisle is the time for two moves). With an increasing size of the system, this constant time can be neglected (see Zaerpour *et al.* (2017)).

A5: *We neglect the constant time required, if any, to create a virtual aisle for a requested unit load.*

As a result, for a system where the I/O point is at the lower left corner, the retrieval time of a unit load at location (x, y) of a single-level live-cube storage system equals the Manhattan distance (in time):

$$t(x, y) = x + y. \qquad (5)$$

Based on the retrieval time function (Equation (5)), a triangular-in-time shape appears to be optimal for a live-cube system for any given capacity. However, such a system is not very practical and much more costly (for a given storage capacity) than a rectangular system.

A6: *We only consider rectangular live-cube compact storage systems.*

In a multi-level live-cube storage system, a lift takes care of the vertical movement. When idle, the lift waits at the lower left corner of the system (i.e., I/O point). Assume (x, y, z) represents a location (in units of time) where z refers to the coordinate of each level (in units of time) in the height direction.

The retrieval time of a unit load consists of the following two components:

1. The time needed to bring the unit load to the lift. Since the movements of shuttles at each level are independent of the movement of the lift, this time equals the maximum of the time to move the unit load to the lift at the same level ($x + y$) and the time needed for the lift to go from the I/O point to the unit load's level (z).
2. The time needed for the lift to return to the I/O point when it has the unit load (z).

Thus, the retrieval time of a unit load located at (x, y, z) for a multi-level live-cube system can be estimated by Equation (6):

$$t(x, y, z) = \max\{x + y, z\} + z. \qquad (6)$$

In order to evaluate the performance of a live-cube system with two classes, we must derive the expected value of the retrieval time of an arbitrary unit load in the first and second
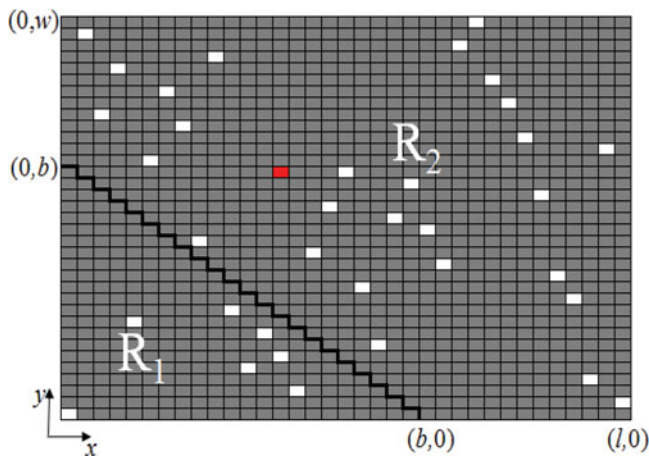
Figure 3. A two-class single-level live-cube system with a first zone boundary.

zones. Figure 3 shows a top view of a single-level live-cube system with two storage classes. For the sake of illustration, we assume that shuttle speeds in the x and y directions are equal and normalized. Then the boundary (bold line) divides the system into two zones; the first zone R_1 includes locations whose retrieval time is less than or equal to b and the second zone R_2 includes locations whose retrieval time is greater than b. In other words, $R_1 = \{(x, y)|x + y \leq b\}$ and $R_2 = \{(x, y)|x + y > b\}$. We consider a system with sufficient empty locations on each level to create virtual aisles (see assumption A4). In the next section, we derive closed-form formulas for the expected retrieval time of a multi-level live-cube system.

3. Analytical model for the expected retrieval time of a live-cube system

In this section, we analytically derive the expected retrieval times for the first and second zones of a two-class live-cube system. The first step is to locate the first zone boundary within a specific configuration of a live-cube system. Several cases can be distinguished, each with a different shape of the first or second zone compared with other cases. In total, 36 cases are obtained. The next step is to divide each case into sub-cases to calculate the expected retrieval time for each sub-case.

As the first step, we obtain all possible shapes of the first and second zones. The boundary B is a set of locations that can

be defined as $B = \{(x, y, z)| \max\{x + y, z\} + z = b\}$. Therefore, the first zone is a set of locations that can be defined as $R_1 = \{(x, y, z)| \max\{x + y, z\} + z \leq b \ \& \ x, y, z \geq 0\}$. However, $\max\{x + y, z\} + z \leq b$ can be split into two inequalities as follows:

$$x + y + z \leq b \ \text{if} \ x + y \geq z,$$

$$2z \leq b \ \text{if} \ x + y < z.$$

The above inequalities, together with $x, y, z \geq 0$, form a truncated pyramid-shaped polytope, as shown in Figure 4(a). This polytope again has to be truncated from different angles by system planes (Figure 4(b)), depending on the position of the parameters l, w, h, and b. Therefore, we can obtain several different shapes for the first and second zones, depending on the position of the first zone boundary and system dimensions.

In Section 3.1, we explain the general procedure for obtaining all possible shapes. For the lengthy detailed procedure, we refer to our working paper (Zaerpour et al., 2017).

3.1. Hierarchical decomposition procedure for shapes with differently shaped R_1 or R_2

In Figure 4(a), we have the planes $z = b/2$ and $x + y + z = b$, whereas in Figure 4(b), we have the planes $z = h$ and $y = w$ and $x = l$. Following a hierarchical procedure, we first consider both horizontal planes in the z-direction (i.e., $z = b/2$ and $z = h$). Two situations are possible depending on the values of b and h: $b/2 \leq h$ and $b/2 > h$. Assuming that the constraints defined by the other planes in Figure 4(b) are not effective, we obtain two different shapes for the second zone, as shown in Figure 5(a) and 5(i) corresponding to $b/2 \leq h$ and $b/2 > h$, respectively. Now let us only consider Figure 5(a). In the y-direction, the shape has two corner points: $(0, b/2, b/2)$ and $(0, b, 0)$. The plane $y = w$ can be positioned differently depending on the value of w and b as follows: $w > b$ (still Fig. 5(a)), $b/2 < w \leq b$ (Fig. 5(b)), $w \leq b/2$ (Fig. 5(d)). The next step is to consider the plane $x = l$ in the x-direction. Let us consider only one of the possibilities obtained so far, which is $b/2 \leq h$ and $w > b$ (still Fig. 5(a)). Figure 5(a) has two corner points in the x-direction: $(b/2, 0, b/2)$ and $(b, 0, 0)$. The plane $x = l$ can be positioned differently depending on the value of l and b as follows: $l > b$ (still Fig. 5(a)), $b/2 < l \leq b$ (not feasible since we have $w > b$

(a)

(b)
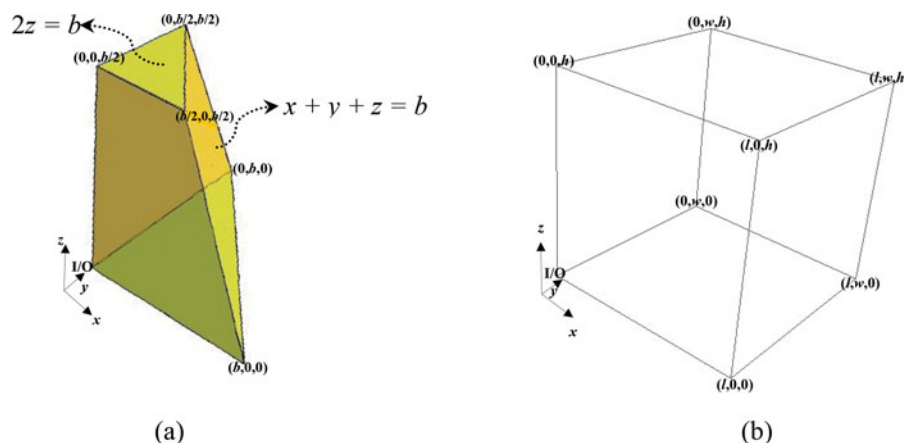
Figure 4. (a) The first zone formed by $x + y + z \leq b$ and $2z \leq b$; and (b) cubic shape of a live-cube system.
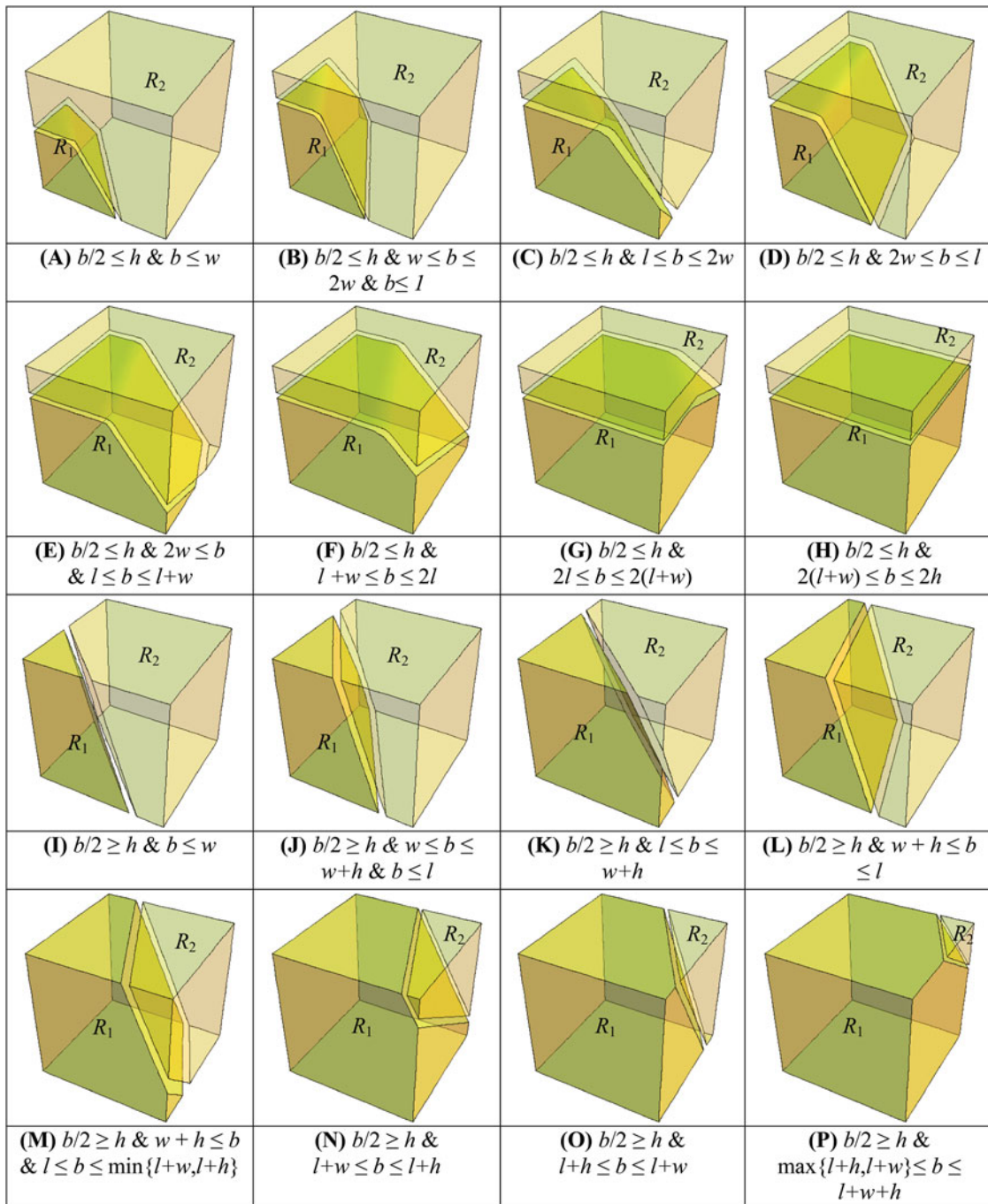
Figure 5. Cases A to P with their corresponding shapes of first and second zones.

and also $l \geq w$), $l \leq b/2$ (not feasible for a similar reason). This hierarchical analysis leads to a tree with each node representing a specific configuration and first zone boundary while some nodes are infeasible (see online supplement). In the illustrative example, only one feasible case ($b/2 \leq h$, $w > b$, $l > b$: Fig. 5(a)) is eventually obtained.

In total 16 different cases can be obtained with differently shaped R_1 or R_2 (see Fig. 5). We denote these 16 cases in an alphabetical order by cases A, B, C , . . . , P.

In order to calculate the volume of the first zone in each case, we consider the base of the solid to be in the yz-plane. Then the function $\min\{l, b - y - z\}$ can be integrated over these boundaries: $0 \leq y \leq w$, $0 \leq z \leq h$, $y + z \leq b$, $z \leq b/2$. Depending on

the shape of the first zone in each case, every boundary might need to be split into several sub-boundaries.

The expected retrieval time of an arbitrary unit load in the first ($E[T^1]$) and second ($E[T^2]$) zones of a live-cube storage system can be calculated by using Equations (7) and (8), respectively:

$$E[T^1] = \int_{t=0}^{b} tf^1(t)\,dt, \tag{7}$$

$$E[T^2] = \int_{t=b}^{\max\{l+w,h\}+h} tf^2(t)\,dt, \tag{8}$$

where b represents the zone boundary parameter, and $f^i(t)$ represents the probability density function of the retrieval time t for zone i ($i = 1, 2$). The cumulative distribution function $F^i(t)$ for $i = 1$ and 2 can be calculated using Equations (9) and (10), respectively:

$$F^1(t) = P(T(X, Y, Z) \leq t)$$
$$= \frac{\text{volume of } \{(x, y, z)|t(x, y, z) \leq t, t \leq b\}}{\text{volume of the first zone}}, \quad (9)$$

$$F^2(t) = P(b \leq T(X, Y, Z) \leq t)$$
$$= \frac{\text{volume of } \{(x, y, z)|b \leq t(x, y, z) \leq t\}}{\text{volume of the second zone}}. \quad (10)$$

In order to calculate $E[T^1]$ and $E[T^2]$, each of 16 cases again needs to be split into at most four sub-cases depending on the system configuration. In total, 36 complementary sub-cases can be considered, each corresponding to a unique $E[T]$ formula. In Section 3.2, we explain the detailed procedure to derive $E[T^1]$ and $E[T^2]$ where case A ($b/2 \leq h$ and $b \leq w$) and configuration $h \leq w$ are considered (i.e., sub-case A1). Then, in Section 3.3 we give all 35 other complementary sub-cases and we discuss all of the sub-cases generally.

3.2. Computation of E[T] for sub-case A1

In this section, we give the detailed procedure of calculating $E[T]$ for one of the sub-cases of case A (sub-case A1: $b \leq 2h$, $b \leq w$, and $h \leq w$). Based on Equation (4), $E[T_{A1}]$ can be calculated as follows:

$$E[T_{A1}] = \left(\frac{7b^3}{48hlw}\right)^{\frac{2s}{1+s}} \frac{3b}{4} + \left(1 - \left(\frac{7b^3}{48hlw}\right)^{\frac{2s}{1+s}}\right)$$
$$\times \frac{21b^4 - 8h\left(h^3 + 12hlw + 12lw(l + w)\right)}{4\left(7b^3 - 48hlw\right)}, \quad (11)$$

where

$$G_1 = \frac{7b^3}{48hlw}, \quad E[T^1_{A1}] = \frac{3b}{4},$$

and

$$E[T^2_{A1}] = \frac{21b^4 - 8h\left(h^3 + 12hlw + 12lw(l + w)\right)}{4\left(7b^3 - 48hlw\right)}.$$

Now, the derivation of all components G_1, $E[T^1_{A1}]$, and $E[T^2_{A1}]$ can be explained. Figure 6 shows the shape of the first and second zones for sub-case A1.

Based on Equations (9) and (10), we first need to calculate the volume of the first and second zones. The volume of the first zone (V^1) can be obtained by integrating the function $\min\{l, b - y - z\}$ over the boundaries $0 \leq y \leq b - z$ and $0 \leq z \leq b/2$. In this case $\min\{l, b - y - z\}$ always equals $b - y - z$. Therefore, the volume of the first zone (V^1) is given by

$$V^1_{A1}(b) = \int_{z=0}^{b/2} \int_{y=0}^{b-z} (b - y - z)dydz = 7b^3/48. \quad (12)$$

The second zone includes the locations of the system that were not assigned to the first zone. Therefore, the volume of the
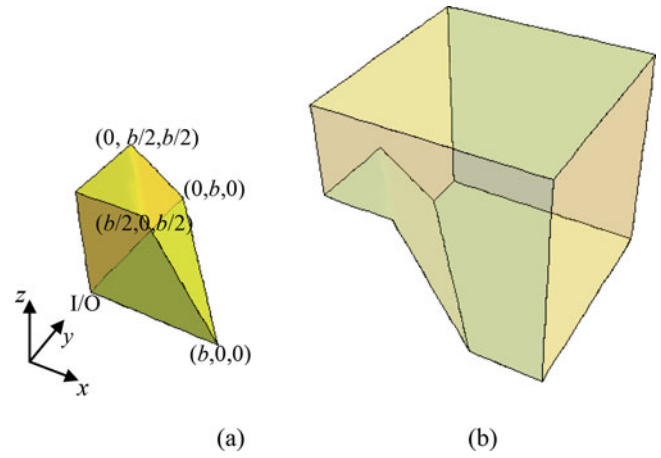

Figure 6. (a) The first zone and (b) the second zone of sub-case A1.

second zone (V^2) is the volume of the system minus the volume of the first zone; that is,

$$V^2_{A1}(b, l, w, h) = wlh - 7b^3/48. \quad (13)$$

G_1 can be obtained by dividing the volume of the first zone ($7b^3/48$) by the volume of the system (lwh); i.e., $G_1 = 7b^3/48lwh$.

In order to calculate $E[T^1_{A1}]$ and $E[T^2_{A1}]$, we first give the following definition:

Definition 1. (*Critical retrieval time*): The critical retrieval time is a time instant t at which the region $T \leq t$ in the first zone or the region $b \leq T \leq t$ in the second zone changes shape, resulting in a different volume formula. ▲

It can be shown that the following values are the critical retrieval times for sub-case A1:

$$w, l, 2h, w + h, l + h, w + l, l + w + h. \quad (14)$$

However, the conditions of sub-case A1 ($b/2 \leq h$, $b \leq w$, $h \leq w$) are not sufficient to arrange these critical retrieval times. In order to be able to arrange critical retrieval times, sub-case A1 needs again to be divided into five different sub-sub-cases as follows:

- sub-sub-case A11: sub-case A1 ($b/2 \leq h$, $b \leq w$, $h \leq w$) plus $l \leq 2h$,
- sub-sub-case A12: sub-case A1 ($b/2 \leq h$, $b \leq w$, $h \leq w$) plus $w \leq 2h$ and $2h < l \leq w + h$,
- sub-sub-case A13: sub-case A1 ($b/2 \leq h$, $b \leq w$, $h \leq w$) plus $w \leq 2h$ and $l > w + h$,
- sub-sub-case A14: sub-case A1 ($b/2 \leq h$, $b \leq w$, $h \leq w$) plus $w > 2h$ and $2h < l \leq w + h$, and
- sub-sub-case A15: sub-case A1 ($b/2 \leq h$, $b \leq w$, $h \leq w$) plus $w > 2h$ and $l > w + h$.

Now it is possible to arrange the critical retrieval times for each of these five sub-sub-cases. One possibility for sub-case A1 is when $l \leq 2h$ (sub-sub-case A11). Therefore, we can arrange the critical retrieval times as follows:

$$w \leq l \leq 2h \leq h + w \leq h + l \leq l + w \leq l + w + h. \quad (15)$$

Now we can calculate $E[T^1]$ and $E[T^2]$ for sub-sub-case A11 ($b/2 \leq h$, $b \leq w$, $h \leq w$, $l \leq 2h$).
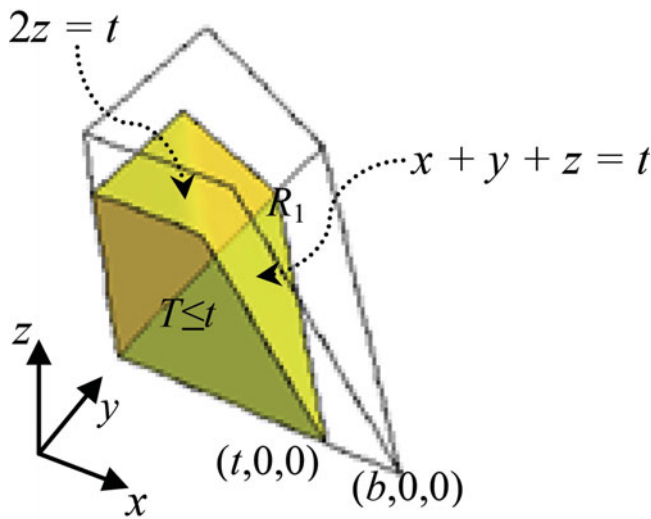
$2z = t$

$x + y + z = t$

R_1

$T \leq t$

z

y

x

$(t, 0, 0)$ $(b, 0, 0)$

Figure 7. Region $T \leq t$ in the first zone of sub-sub-case A11.

3.2.1. Computation of $E[T^1_{A11}]$

In order to calculate $E[T^1_{A11}]$ we first need to derive the cumulative distribution function of the random variable T by using Equation (9). Based on Equation (15), we have $w \leq 2h$, and so $0 \leq b \leq w$. Therefore, the only possible situation for retrieval time t in the first zone is when $0 \leq t \leq b$. Figure 7 shows the shape of the region $T \leq t$ in the first zone.

In this case, the shape of region $T \leq t$ is exactly the same as the shape of the first zone. Therefore, the volume of region $T \leq t$ is given by

$$\int_{z=0}^{t/2} \int_{y=0}^{t-z} (t - y - z) dy dz = 7t^3/48.$$

The cumulative distribution function for the first zone can now be derived by using Equation (9). By taking the derivative, the probability density function is obtained. Therefore, we have

$$F^1_{A11}(t) = t^3/b^3,$$

$$f^1_{A11}(t) = \frac{dF^1_{A11}(t)}{dt} = 3t^2/b^3.$$

Consequently, $E[T^1_{A11}]$ is given by

$$E[T^1_{A11}] = \int_0^b (3t^3/b^3) dt = \frac{3b}{4}. \tag{16}$$

In fact, $E[T^1_{A1}] = E[T^1_{A11}] = E[T^1_{A12}] = E[T^1_{A13}] = E[T^1_{A14}] = E[T^1_{A15}]$, since it can be shown that the other four sub-sub-cases (A12, . . . , A15) lead to a similar closed-form formula as Equation (16). For the proof, we refer to our working paper.

3.2.2. Computation of $E[T^2_{A11}]$

Based on Equation (15), seven different positions for the retrieval time t in sub-sub-case A11 are possible; they are $b \leq t < w$; $w \leq t < l \ldots l + w \leq t \leq l + w + h$. Each of these seven boundaries corresponds to one of the regions $b \leq T \leq t$ in Figure 8. Figure 8 shows that the region $b \leq T \leq t$ changes shape between boundaries. Therefore, we need to calculate the

volume formula and correspondingly the cumulative distribution and density function for eacdh shape. We here explain the procedure for Figures 8(a), 8(b), and 8(c).

In Figure 8(a), we have $b \leq t < w$. Since $t < w$, the shape does not touch the $y = w$ plane of the cube. In addition, since $w \leq l$, the shape does not touch the $x = l$ plane of the cube either. Furthermore, $z = t/2$ represents the top surface of the shape. However, $t < w$ and also $w < 2h$ (see Equation (15)) and therefore $t < 2h$. Hence, the plane $z = t/2$ of the shape does not touch the plane $z = h$ of the cube.

In Figure 8(b), $w \leq t < l$. Since $w \leq t$, the shape touches the $y = w$ plane of the cube. The point $(t - w, w, 0)$ in the $y = w$ plane has a retrieval time equal to $t(t - w + w)$, which is greater than w. The explanation for the shape of the polytope in x and z directions is similar to the previous shape.

In Figure 8(c), $l \leq t < 2h$. Since $l \leq t$, the shape touches the $x = l$ plane of the cube. The corner point $(l, t - l, 0)$ of the shape has retrieval time $t(t - l + l)$, which is greater than l. The explanation for the shape of polytope in y and z directions is similar to the previous shape.

The other shapes in Figure 8 can be explained similarly.

We now derive the volumes of the first three shapes in Figure 8 by considering the base of the shape to be in the yz-plane. In Figure 8(a), the region $b \leq T \leq t$ can be formed by removing the first zone from the region $0 \leq T \leq t$. The volume of the region $0 \leq T \leq t$ is $7t^3/48$ and therefore the volume of region $b \leq T \leq t$ can be calculated by

$$\int_{z=0}^{t/2} \int_{y=0}^{t-z} (t - y - z) dy dz - 7b^3/48 = 7(t^3 - b^3)/48.$$

In Figure 8(b), we derive the volume of the region $0 \leq T \leq t$ and then subtract the volume of the first zone. For the region $0 \leq T \leq t$, y and z are bounded as follows: $0 \leq y \leq \min\{w, t - z\}$, $0 \leq z \leq t/2$. The volume of the region $0 \leq T \leq t$ is given by

$$\int_{z=0}^{t/2} \int_{y=0}^{\min\{w, t-z\}} (t - y - z) dy dz.$$

Figure 8(b) shows the line $y = t - z$ intersects the $y = w$ plane at the point $(0, w, t - w)$. For any $z \leq t - w$, $\min\{w, t - z\} = w$ and for any $z > t - w$, $\min\{w, t - z\} = t - z$. Therefore, the volume of Figure 8(b), where $w \leq t < l$, is given by

$$\int_{z=0}^{t-w} \int_{y=0}^{w} (t - y - z) dy dz$$

$$+ \int_{z=t-w}^{t/2} \int_{y=0}^{t-z} (t - y - z) dy dz - 7b^3/48$$

$$= \frac{1}{48}(-b^3 - t^3 + 24t(t - w)w + 8w^3).$$

Figure 8(c) is a truncated version of Figure 8(b); the plane $x = l$ has removed a pyramid shaped top in the x-direction. Therefore, volume (10c) = volume (10b) – volume (truncated pyramid). The height of the removed pyramid equals $t - l$, and the base of the pyramid is a right triangle with both legs equaling $t - l$. Therefore, the volume of the removed pyramid equals $(t - l)^3/6$. The resulting volume of Figure 8(c) is given
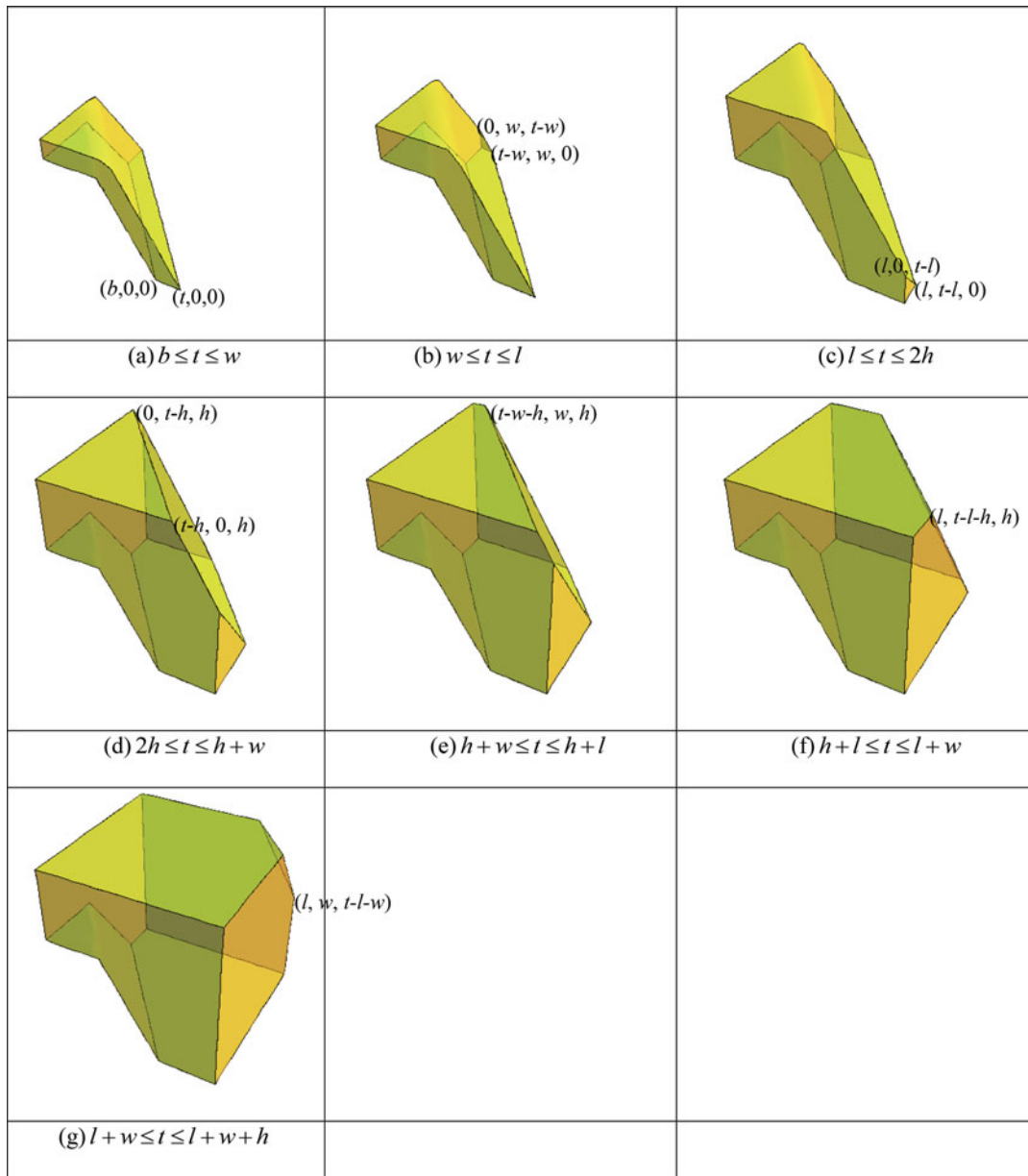
Figure 8. Region of $b \leq T \leq t$ for the second zone of sub-sub-case A11.

by

$$\int_{z=0}^{t-w} \int_{y=0}^{w} (t - y - z) dy dz$$

$$+ \int_{z=t-w}^{t/2} \int_{y=0}^{t-z} (t - y - z) dy dz - \frac{1}{6}(t - l)^3 - 7b^3/48$$

$$= \frac{1}{48} \left(-b^3 - t^3 - 8(t - l)^3 + 24t(t - w)w + 8w^3 \right).$$

The cumulative distribution function of the second zone for each shape in Figure 8 can be derived by using Equation (10). By taking the derivative, the probability density function is obtained. Corresponding to Figures 8(a) to (c), the cumulative distribution and density functions are given by

$$F^2(t) = \left(7(t^3 - b^3)/48 \right) / \left(wlh - 7b^3/48 \right) \quad \text{if } b \leq t < w,$$

$$f^2(t) = \frac{d(F^2)}{dt} = (21t^2)/(48hlw - 7b^3) \quad \text{if } b \leq t < w,$$

$$F^2(t) = \left(\frac{1}{48} \left(-b^3 - t^3 + 24t(t - w)w + 8w^3 \right) \right) \Bigg/$$

$$(wlh - 7b^3/48) \quad \text{if } w \leq t < l,$$

$$f^2(t) = \frac{d(F^2)}{dt} = \frac{-3t^2 + 48wt - 24w^2}{48hlw - 7b^3} \quad \text{if } w \leq t < l,$$

$$F^2(t) = \frac{1}{48} \left(-b^3 - t^3 - 8(t - l)^3 + 24t(t - w)w + 8w^3 \right) /$$

$$(wlh - 7b^3/48) \quad \text{if } l \leq t < 2h,$$

$$f^2(t) = \frac{d(F^2)}{dt}$$

$$= \frac{-3t^2 - 24(t - l)^2 + 48wt - 24w^2}{48hlw - 7b^3} \quad \text{if } l \leq t < 2h.$$

The probability density function for other boundaries in Figure 8 can be calculated similarly. This results in

$$
f^2_{A11} =
\begin{cases}
(21t^2)/(48hlw - 7b^3) & \text{if } b \le t < w, \\[2mm]
\dfrac{-3t^2 + 48wt - 24w^2}{48hlw - 7b^3} & \text{if } w \le t < l, \\[3mm]
\dfrac{-3t^2 - 24(t-l)^2 + 48wt - 24w^2}{48hlw - 7b^3} & \text{if } l \le t < 2h, \\[3mm]
\dfrac{-3h^2 - 3(l-t)^2 + 6ht - 3t^2 + 3wt + 3(t-w)w}{6(wlh - 7b^3/48)} \\[1mm]
& \text{if } 2h \le t < w + h, \\[3mm]
\dfrac{-\dfrac{1}{2}(l-t)^2 + hw}{wlh - 7b^3/48} & \text{if } w + h \le t < l + h, \\[3mm]
\dfrac{h^2 + 2h(l-t+w)}{2(wlh - 7b^3/48)} & \text{if } l + h \le t < l + w, \\[3mm]
\dfrac{(h+l-t+w)^2}{2(wlh - 7b^3/48)} & \text{if } l + w \le t \le l \\[1mm]
& \qquad + w + h, \\[3mm]
0 & \text{otherwise.}
\end{cases}
\tag{17}
$$

Consequently, $E[T^2_{A11}]$ can be calculated by

$$
E[T^2_{A11}] = \left(\frac{48}{48lwh - 7b^3} \right)
$$

$$
\times
\begin{pmatrix}
\displaystyle\int_b^w \left(t\left(\frac{21t^2}{48}\right) \right) dt + \int_w^l \left(t\left(\frac{-3t^2 + 48wt - 24w^2}{48}\right) \right) dt \\[3mm]
+ \displaystyle\int_l^{2h} \left(t\left(\frac{-3t^2 - 24(t-l)^2 + 48wt - 24w^2}{48}\right) \right) dt \\[3mm]
+ \displaystyle\int_{2h}^{w+h} \left(t\left(-\frac{1}{2}(t-l)^2 + \frac{1}{6}\left(-3h^2 + 6ht - 3t^2\right)\right.\right. \\[3mm]
\left.\left. + \frac{tw}{2} + \frac{1}{2}(t-w)w\right) \right) dt \\[3mm]
+ \displaystyle\int_{w+h}^{l+h} \left(t\left(-\frac{1}{2}(t-l)^2 + hw\right) \right) dt \\[3mm]
+ \displaystyle\int_{l+h}^{l+w} \left(t\left(\frac{h^2 + 2h(l-t+w)}{2}\right) \right) dt \\[3mm]
+ \displaystyle\int_{l+w}^{l+w+h} \left(t\left(\frac{(h+l-t+w)^2}{2}\right) \right) dt
\end{pmatrix}
$$

$$
= \frac{21b^4 - 8h(h^3 + 12hlw + 12lw(l+w))}{4(7b^3 - 48lwh)}.
\tag{18}
$$

In fact, $E[T^2_{A1}] = E[T^2_{A11}] = E[T^2_{A12}] = E[T^2_{A13}] = E[T^2_{A14}] = E[T^2_{A15}]$, since it can be shown that the other four sub-sub-cases (A12 , . . . , A15) lead to similar closed-form formula as Equation (18). For the proof, we refer to our working paper.

3.3. Discussion on the computation of E[T] for other sub-cases

Sixteen different cases (cases A , . . . , P) have been considered based on the shapes of the first and second zones, which are illustrated in Figure 5. However, it is necessary to decompose each case into at most four sub-cases based on system configurations as follows:

- Configuration 1. $h \le w$,
- Configuration 2. $w \le h \le l$,
- Configuration 3. $l \le h \le l + w$, and
- Configuration 4. $l + w \le h$.

Therefore, a total of 36 sub-cases can be obtained (e.g., sub-case A1 discussed in Section 3.2), each corresponding to a specific closed-form formula for $E[T]$. Table 2 gives all 36 possible sub-cases. Any sub-case XY corresponds to case X and configuration Y (e.g., case A and configuration 1 results in sub-case A1). For each pair of adjacent sub-cases, the closed-form formulas for $E[T]$ coincide at the boundaries. For instance, the closed-form formulas for $E[T]$ for the two sub-cases A1 and B1 result in the same value if $b = w$.

We now explain the reason for decomposing each case into at most four sub-cases through an illustrative example. We consider sub-case A1 ($b/2 \le h$, $b \le w$, $h \le w$) described in Section 3.2 and sub-case A2 ($b/2 \le h$, $b \le w$, $w \le h \le l$). The shapes of the first and second zones for both sub-cases are similar. Therefore, we expect that they both lead to the same closed-form formula. However, the closed-form formulas for these two sub-cases are different. It is necessary to examine the critical retrieval times. Equation (14) gives the critical retrieval times for sub-case A1 and Equation (19) gives the critical retrieval times for sub-case A2:

$$
l, \ w, \ 2h, \ 2w, \ l + h, \ w + l, \ l + w + h. \tag{19}
$$

Comparing Equations (14) and (19) shows that even though the shapes of the first and second zones in sub-cases A1 and A2 are similar, they have different critical retrieval times (e.g., $w + h$ in sub-case A1 and $2w$ in sub-case A2). Different critical retrieval times lead to different volume formulas in the derivation process. Therefore, different cumulative distribution functions, different density functions, and consequently different closed-form formulas for $E[T]$ are obtained. Comparing sub-cases A1 and A2, identical expressions for $E[T^1]$ are obtained for both sub-cases; however, $E[T^2]$, and consequently $E[T]$, will be different.

In addition, the four configurations are not always feasible for all cases. Consider, for example, case D ($b/2 \le h$, $w \le b/2$, $b \le l$) together with configuration 1 ($h \le w$). In case D, $b/2 \le h$ and $w \le b/2$, which means $h \ge w$. This is inconsistent with configuration 1, which is $h \le w$. As can be seen from Table 2, sub-case D1 is not feasible and is therefore blank. Similar to sub-case A1 in Section 3.2, each sub-case is decomposed into a maximum of five sub-sub-cases to derive the closed-form formulas. However, similar to sub-case A1, the obtained closed-form formulas are the same for all sub-sub-cases. The derivation procedure for all 36 sub-cases is very tedious and exhaustive. However, the results obtained are simple to use.

Table 2. All sub-cases, each corresponding to a specific $E[T]$ formula*.

	Case			
	Configuration 1. $h \leq w$	Configuration 2. $w \leq h \leq l$	Configuration 3. $l \leq h \leq l + w$	Configuration 4. $l + w \leq h$
A $(b/2 \leq h \ \& \ b \leq w)$	A1	A2	A3	A4
B $(b/2 \leq h \ \& \ w \leq b \leq 2w \ \& \ b \leq l)$	B1	B2	B3	B4
C $(b/2 \leq h \ \& \ l \leq b \leq 2w)$	C1	C2	C3	C4
D $(b/2 \leq h \ \& \ 2w \leq b \leq l)$	—	D2	D3	D4
E $(b/2 \leq h \ \& \ 2w \leq b \ \& \ l \leq b \leq l + w)$	—	E2	E3	E4
F $(b/2 \leq h \ \& \ l + w \leq b \leq 2l)$	—	F2	F3	F4
G $(b/2 \leq h \ \& \ 2l \leq b \leq 2(l + w))$	—	—	G3	G4
H $(b/2 \leq h \ \& \ 2(l + w) \leq b \leq 2h)$	—	—	—	H4
I $(b/2 \geq h \ \& \ b \leq w)$	I1	—	—	—
J $(b/2 \geq h \ \& \ w \leq b \leq w + h \ \& \ b \leq l)$	J1	—	—	—
K $(b/2 \geq h \ \& \ l \leq b \leq w + h)$	K1	—	—	—
L $(b/2 \geq h \ \& \ w + h \leq b \leq l)$	L1	L2	—	—
M $(b/2 \geq h \ \& \ w + h \leq b \ \& \ l \leq b \leq \min\{l + w, l + h\})$	M1	M2	—	—
N $(b/2 \geq h \ \& \ l + w \leq b \leq l + h)$	—	N2	—	—
O $(b/2 \geq h \ \& \ l + h \leq b \leq l + w)$	O1	—	—	—
P $(b/2 \geq h \ \& \ \max\{l + h, l + w\} \leq b \leq l + w + h)$	P1	P2	P3	—

Note. *The closed-form formulas for sub-cases A1 , . . . , P3 can be found in Appendix A, Tables A1 to A3.

The volume of the first zone (V_1), $E[T^1]$ and $E[T^2]$ for each sub-case, is given in Appendix A, Tables A1, A2, and A3, respectively. Tables A2, A3, and A4 can be used as a reference to instantly evaluate the performance of any two-class-based live-cube compact storage system with any configuration and first zone boundary. According to Equation (4), the expected retrieval time for each sub-case can be calculated by

$$E[T] = G_1^{2s/(s+1)} E[T^1] + \left(1 - G_1^{2s/(s+1)}\right) E[T^2].$$

For example, for case B2, G_1, $E[T^1]$, $E[T^2]$, and $E[T]$ are as follows:

$$G_{B2} = \frac{1}{48lwh}(-b^3 + 24b(b - w)w + 8w^3),$$

$$E[T_{B2}^1] = \frac{3b^4 - 64b^3 w + 48b^2 w^2 - 8w^4}{4b^3 - 96b^2 w + 96bw^2 - 32w^3},$$

$$E[T_{B2}^2] = \frac{3b^4 - 64b^3 w + 48b^2 w^2 + 16w(2h^3 + h^2(6l - 3w) - w^3 + 2h(3l^2 + 3lw + w^2))}{4(b^3 - 24b^2 w + 48hlw + 24bw^2 - 8w^3)},$$

$$E[T_{B2}] = \left(\frac{1}{48lwh}\left(-b^3 + 24b(b - w)w + 8w^3\right)\right)^{\frac{2s}{s+1}} \left(\frac{3b^4 - 64b^3 w + 48b^2 w^2 - 8w^4}{4b^3 - 96b^2 w + 96bw^2 - 32w^3}\right)$$

$$+ \left(1 - \left(\frac{1}{48lwh}\left(-b^3 + 24b(b - w)w + 8w^3\right)\right)^{\frac{2s}{s+1}}\right)$$

$$\times \left(\frac{3b^4 - 64b^3 w + 48b^2 w^2 + 16w(2h^3 + h^2(6l - 3w) - w^3 + 2h(3l^2 + 3lw + w^2))}{4(b^3 - 24b^2 w + 48hlw + 24bw^2 - 8w^3)}\right).$$

For any configuration (l, w, h) and zone boundary (b), the corresponding sub-case can be found in Table 2 and the closed-form formula can be constructed similarly.

4. Numerical results

In this section, we evaluate the accuracy of the closed-form formulas for estimating the average response time of real live-cube systems. To obtain the closed-form formulas, a continuous system is assumed; however, in reality the systems are discrete. In addition, for each instance tested, the performance of the two-class-based storage policy is compared with a random storage policy and a "cuboid" two-class-based storage policy (a straightforward, practical implementation of a two-class policy with rectangular-cube-shaped first zone). Compared with the 16 cases in Figure 5, under a cuboid two-class-based policy, the first zone does not change shape when the first zone increases in size and when the system configuration changes (the dimension ratios of the first zone are equal to the dimension ratios of the system; i.e., $l_1/w_1 = l/w$, $l_1/h_1 = l/h$). The system is analyzed in Appendix B.

As we can expect that the continuous approximation is better for large-scale systems, we also include small-sized systems.

Our base example is based on a live-cube system from a South Korean company that produces live-cube parking systems. Although the system can be designed to be in any desired size, we here focus on a medium-sized live-cube parking system. Table 3 shows the input parameters describing the live-cube storage system. We consider a typical moderate ABC curve in practice, which is 20–80% (20% of inventoried products represent 80% of total demand in number of unit loads). The corresponding skewness parameter s can be calculated using Equation (1). Thirty percent of the closest storage locations to

Table 3. Parameters describing storage system and storage policy.

Fixed parameters	Data	
Size of a standard vehicle (mm)	Height = 1550, width = 5160, length = 2100*	
Size of a storage location (mm)	Height = 2925, width = 6400, length = 3250	
Shuttle speed in x-direction (v_x) (m/min)	45	
Shuttle speed in y-direction (v_y) (m/min)	100	
Lift speed (v_z) (m/min)	90	
Size of storage location (sec)	Height = 1.95, width = 3.80, length = 4.33	
Varying parameters	*Base example data*	*Range for scenarios*
Size of system (sec)	Height = 13.65, width = 15.2, length = 21.65	
Size of system (m)	Height = 23.4, width = 32, length = 19.5	
First zone size (percentage of system size)	30%	[20%, 100%]
ABC curve (percentage)	20–80%	[20–20%, 20–90%]
Capacity of the system (no. of parking slots)**	192	[100, 4000]
Length/width (no. of tiers)	1.2	[0.25, 4]
Height (no. of tiers)	8	[6, 30]

Notes. *Length and width denote the size in x and y directions, respectively.
**Capacity of the system = total slots (Length × Width × Height = 6 × 5 × 8 = 240 (in number of tiers)) – Empty slots required to create virtual aisles (empty slots per level × Height in number of tiers = 6 × 8).

the I/O point are dedicated to the first zone, and the remaining 70% of locations accommodate the vehicles that belong to the second class and stay in the system for a longer period of time. In order to calculate the expected retrieval time by using closed-form formulas, the corresponding sub-case has to be considered. For any given configuration and any volume of the first zone, the boundary parameter b can be obtained by using the volume formula of the first zone; i.e., $V^1(b)/V = G_1$. Since the sub-cases are complementary, exactly one case can be considered for any configuration and first zone boundary. The results of Zaerpour (2017) are used to calculate the expected retrieval time of a live-cube system under random storage. The closed-form formulas for the expected retrieval of two-class-based storage with a cuboid first zone are given in Appendix B.

First, we present the results for the base example. Then, we perform a sensitivity analysis to test the quality of closed-form formulas for different sources of variation in the input parameters. In each experiment, we vary one of the parameters of the base example over five different alternative values.

Table 4 shows the results for the base example. We obtain the expected retrieval time for each instance by considering the probability of requesting each product, the probability of retrieving the requested product from each storage location, and the travel distance from each storage location to the I/O point.

In subsequent tables, we vary system size (Table 5), first zone size (Table 6), the skewness parameter or ABC curve (Table 7), height (Table 8), and shape factor of the system—i.e., L/W (in number of tiers; Table 9)—while the other parameters stay the same. In Table 5, when varying the system size, the number of tiers in the x-direction and y-direction are equal; i.e., $L/W = 1$. In Table 9, when varying the shape factor, the size of the system changes correspondingly.

4.1. Results on the accuracy of the closed-form formulas

Table 4 shows that for our base example the closed-form formula gives a very precise approximation of the expected retrieval time of a medium-sized real discrete system. Tables 5 to 9 show that the closed-form formulas give a very precise approximation of the expected retrieval times of real discrete systems, with errors all less than 4%. In addition, the sensitivity analysis proves that by varying the system parameters, the closed-form formulas can still give very good approximations of the expected retrieval times of real discrete systems, even for extreme cases such as very small-size systems (100 storage locations), very steep ABC curves (e.g., 20–90%), and small sizes of the first zone. Moreover, we observe the following points.

Observation 1: The accuracy of the closed-form formulas increases with an increase in the size of the system (see Table 5). This is because we assume a continuous system in the derivation procedure, whereas the evaluation results are based on a discrete system. The continuity assumption becomes more accurate if the size of the system divided by the size of a storage location is sufficiently large.

Observation 2: The accuracy of the closed-form formulas increases with an increase in size of the first zone (see Table 6). Based on Observation 1, the results of the closed-form formulas are more accurate for a larger system. Therefore, with an increase in size of the first zone, the formula for the first zone gives a result closer to reality. Since we consider a 20–80% ABC curve, the expected retrieval time for the first zone has a higher impact on the total expected retrieval time. Therefore, for a larger first zone, the expected retrieval time of the first zone and, consequently, the expected retrieval time of the system, are closer to the one obtained from a real application.

Table 4. Comparison of the expected retrieval times obtained from the closed-form formula and real discrete system for the base example.

First zone size (%)	ABC curve	Corresponding sub-case	Boundary (b) (sec)	$E[T_D]$ (sec)	$E[T_S]$ (sec)	Gap_S (%)	$E[T_C]$ (sec)	Gap_C (%)	$E[T_R]$ (sec)	Gap_R (%)
30	20–80%	B1	21.17	19.34	19.03	1.60	20.19	4.42	25.57	32.23

Notes. $E[T_x]$ is the expected retrieval time for method x (in seconds), where x = D (Derived continuous closed-form formulas), S (real discrete System), C (a two-class-based system with a Cuboid first zone), R (a system with Random storage). $Gap_x = (|E[T_x] - E[T_D]|)/E[T_D] \times 100\%$, represents the gap between the expected retrieval time of our proposed two-class-based live-cube system obtained using closed-form formulas and expected retrieval time of method x.

Table 5. Results of sensitivity analysis when varying system size.

System size (No. of slots)*	Corresponding sub-case	Boundary (b) (sec)	$E[T_D]$ (sec)	$E[T_S]$ (sec)	Gap_S (%)	$E[T_C]$ (sec)	Gap_C (%)	$E[T_R]$ (sec)	Gap_R (%)
100 (5 × 5 × 4) **	J1	15.38	14.11	13.71	2.80	15.17	7.58	19.22	36.24
500 (10 × 10 × 5)	I1	32.09	29.13	28.80	1.12	31.98	9.81	40.50	39.05
1000 (10 × 10 × 10)	J1	36.60	33.92	33.65	0.81	35.95	5.98	45.53	34.21
2000 (10 × 10 × 20)	C2	47.13	42.94	42.70	0.57	44.77	4.26	56.70	32.04
4000 (10 × 10 × 40)	C3	63.23	61.10	60.85	0.41	68.17	11.57	86.32	41.29

Notes.
* Including empty slots.
**Length × Width × Height in number of tiers.

Table 6. Results of sensitivity analysis when varying first zone size.

First zone size (%)	Corresponding sub-case	Boundary (b) (sec)	$E[T_D]$ (sec)	$E[T_S]$ (sec)	Gap_S (%)	$E[T_C]$ (sec)	Gap_C (%)	$E[T_R]$ (sec)	Gap_R (%)
20	B1	18.37	18.55	18.22	1.79	19.27	3.85	25.57	37.84
40	C1	23.50	20.14	19.88	1.31	21.09	4.69	25.57	26.95
60	K1	27.58	21.73	21.51	1.01	22.74	4.66	25.57	17.69
80	M1	32.88	23.41	23.32	0.39	24.22	3.48	25.57	9.23
100	—	—	25.57	25.49	0.32	25.57	0.00	25.57	0.00

Note.—Means any sub-case or any value for *b*.

Observation 3: The accuracy of the closed-form formulas increases with a decrease in the skewness of the ABC curve (see Table 7). We considered a fixed size (30% of the system size) for the first zone in every instance of Table 7, which means that the closed-form formula of the second zone leads to more accurate results. In addition, if the skewness of the ABC curve decreases, the turnover of the unit loads in the second zone will relatively increase. This increases the weight of the expected retrieval time of the second zone in the total expected retrieval time.

Observation 4: The accuracy the closed-form formulas increases by increasing the height and by departing from an equal length and width ratio (shape factor equal to one; see Tables 8 and 9). This is due to the size of the system increasing in both cases, leading to more precise results from the closed-form formulas.

4.2. Results on the performance of two-class-based storage

The results in Tables 4 to 9 show that our proposed two-class-based storage can significantly reduce the average response time of a live-cube system compared with random storage (up to 55%) and to two-class-based storage with a cuboid first zone (up to 22%). In addition, the implementation of a two-class-based storage policy requires no system configuration modification

and no additional investment in infrastructure. The assignment software operating the live-cube system needs only to distinguish locations with a travel time b to the I/O point and assign incoming loads to a random location either in the first or second zone. Moreover, we make the following observations.

Observation 5: Even with a typical moderate ABC curve (20–80%) and a typical first zone size (30%), our proposed two-class-based storage significantly reduces average response for both large and small system sizes (∼40%) compared with random storage (see Table 5). This reduction is less pronounced (up to 12%) compared with a two-class-based system with a cuboid first zone. In each instance, a more skewed ABC curve and a smaller first zone might even increase this gap further (see Observations 6 and 7). Thus, facility managers are advised to implement the proposed two-class-based storage policy for any system size to further improve the performance of a live-cube system.

Observation 6: By increasing the first zone size, the gap between two-class-based storage and random storage decreases (see Table 6, $Gap_R = 37.84\%$ for first zone size = 20% versus $Gap_R = 0\%$ for first zone size = 100%). Thus, facility managers are advised to dedicate a small number of storage locations close to the I/O point to the first zone (typically less than 20% of the total number of locations). Although obtaining the

Table 7. Results of sensitivity analysis when varying the skewness parameter.

ABC curve (%)	Corresponding sub-case	Boundary (b) (sec)	$E[T_D]$ (sec)	$E[T_S]$ (sec)	Gap_S (%)	$E[T_C]$ (sec)	Gap_C (%)	$E[T_R]$ (sec)	Gap_R (%)
20–90	B1	21.17	17.69	17.21	2.70	18.77	6.11	25.57	44.57
20–70	B1	21.17	20.70	20.37	1.62	21.37	3.22	25.57	23.51
20–50	B1	21.17	22.99	22.73	1.11	23.34	1.54	25.57	11.25
20–30	B1	21.17	24.78	24.57	0.86	24.89	0.44	25.57	3.18
20–20	—	—	25.57	25.49	0.32	25.57	0.00	25.57	0.00

Table 8. Results of sensitivity analysis when varying height.

Height (No. of tiers)	Corresponding sub-case	Boundary (b) (sec)	$E[T_D]$ (sec)	$E[T_S]$ (sec)	Gap_S (%)	$E[T_C]$ (sec)	Gap_C (%)	$E[T_R]$ (sec)	Gap_R (%)
6	B1	18.81	17.47	17.03	2.54	18.49	5.83	23.42	34.02
12	C2	25.01	22.80	22.44	1.59	24.00	5.25	30.39	33.28
18	C3	29.89	28.18	27.77	1.47	30.92	9.69	39.15	38.91
24	E4	34.46	33.45	33.14	0.93	38.92	16.35	49.28	47.34
30	F4	39.15	39.00	38.82	0.47	47.43	21.62	60.07	54.01

Table 9. Results of sensitivity analysis when varying shape factor (length and width in number of tiers).

Shape factor (L/W)	Corresponding sub-case	Boundary (b) (sec)	$E[T_D]$ (sec)	$E[T_S]$ (sec)	Gap_S (%)	$E[T_C]$ (sec)	Gap_C (%)	$E[T_R]$ (sec)	Gap_R (%)
0.25	L1	43.87	41.36	40.84	1.27	48.49	17.23	61.41	48.45
0.5	J1	30.11	28.15	27.53	2.21	30.53	8.46	38.67	37.35
1	C1	22.64	20.76	20.03	3.51	21.64	4.26	27.41	32.03
2	B1	26.30	24.72	24.06	2.68	26.92	8.88	34.09	37.88
4	L1	39.11	37.00	36.32	1.84	43.94	18.76	55.64	50.39

optimal size of the first zone in a two-class-based live-cube system requires further investigation, this result is consistent with the findings of Hausman *et al.* (1976) and Yu and de Koster (2009), who study the optimal configuration and first zone size of automated single-deep and gravity-based compact storage systems, respectively.

Observation 7: By decreasing the skewness of the ABC curve (i.e., less difference between the turnovers of stored products), the gap between our proposed two-class-based storage and the other two storage policies (Gap_R and Gap_C) decreases (see Table 7). This shows that the improvement of the two-class-based storage policy over the other storage policies highly depends on the skewness of the ABC curve (see Table 7). Moreover, in Table 7, when the ABC curve changes from 20–30% to 20–20%, Gap_R reduces from 3.18 to 0.00%. However, when it changes from 20–90% to 20–80%, Gap_R reduces from 44.57 to 32.23%. In conclusion, a two-class-based storage policy pays off when the ABC curve is more skewed (steep).

Observation 8: By increasing the height of the live-cube system, the two-class-based storage becomes more beneficial, as Gap_R and Gap_C increase (see Table 8). In addition, as the length and width of a live-cube system (in number of tiers) differ more from each other (i.e., from $L/W = 1$ to 4 or 0.25), two-class-based storage becomes more favorable compared with random storage and cuboid two-class-based storage (see Gap_R and Gap_C in Table 9). This is mainly because the system avoids extreme situations where high turnover products are assigned to locations very far from the I/O point.

5. Conclusions and future research

We study a next generation of storage systems: live-cube compact storage systems. These systems are increasingly being used in service sectors such as automated parking systems, warehouses, and container terminals. A live-cube system can realize a high storage density, since virtually no transportation aisles are needed. The system can rapidly respond to customer orders, due to independent and simultaneous movements of its components in three-dimensional space. One of the most important performance measures is the customer response time. We consider a two-class-based storage policy, which significantly reduces response times compared with random storage. We derive closed-form formulas to calculate the expected retrieval time of a two-class-based live-cube system for any system configuration, zone boundary, and ABC curve. In order to obtain the closed-form formulas, the system needs to be decomposed into multiple cases. However, eventually they can be summarized in simple closed-form formulas, which can be used to instantly evaluate the performance of any two-class-based live-cube system. In order to evaluate the quality of these closed-form

formulas (obtained using a continuous-space approximation), a discrete live-cube system in a real-life setting is used. The results show that the closed-form formulas approximate the expected retrieval time of a discrete system with high precision; errors are less than 4% for all instances tested. With increasing system size, skewness parameter, and first zone size, the approximation becomes more precise. In addition to performance evaluation of two-class-based live-cube systems, the closed-form formulas can be used as a reference for further research on live-cube systems, such as optimizing system configurations and first zone boundaries. Moreover, the numerical results show that our proposed two-class-based storage policy can significantly improve the average response time to customers compared with a random storage policy (up to 55%) and a cuboid two-class-based storage policy (up to 22%). The improvement is more noteworthy when the ABC curve is more skewed and the first storage zone is relatively small.

This article is one of the first to study the new live-cube systems. It is possible to optimize the system dimensions and zone boundary using the obtained closed-form formulas. In order to optimize the system dimensions and zone boundary, the optimal solution of each sub-case needs to be obtained. The global optimal solution can then be found by comparing the optimal solutions of all sub-cases. It is also of interest to study the impact on makespan of optimally sequencing a group of retrievals. We know from AS/RS literature that savings of 20–70% can be achieved compared to first-come first-served sequencing (Han *et al.*, 1987; Yu and de Koster, 2012). As shuttles can move unit loads on different levels simultaneously, improvements might even be larger for live-cube compact storage systems. While we have studied live-cube compact storage systems with lifts, results for other live-cube compact storage systems with different vertical movement mechanisms may also prove worthwhile investigating.

Funding

Notes on contributors

Nima Zaerpour is an Assistant Professor of Operations and Supply Chain Management at the College of Business Administration, California State University San Marcos, California. He received his Ph.D. in Operations Management from Rotterdam School of Management, Erasmus University, The Netherlands, in 2013. Prior to joining California State University, he was an Assistant Professor at VU University Amsterdam. In 2012, he was a visiting scholar at the School of Industrial and Systems Engineering at Georgia Tech. In 2011, he was a visiting scholar at the School of Management, University of Science and Technology of China. His research has

been published in several journals, including *Production and Operations Management*, *Transportation Science*, *IISE Transactions*, *European Journal of Operational Research*, and *International Journal of Production Research*. His research interests are facility logistics management, distribution logistics management, supply chain management, and terminal operations management, in particular, studying recent innovations in these areas. He serves as a reviewer for journals such as *Operations Research*, *Production and Operations Management*, *Transportation Science*, *IIE Transactions*, *Interfaces*, *IJPE*, *IJPR*, *Omega*, and *OR Spectrum*. He has developed warehousing decision support software and has served as consultant for supply chain and logistics companies.

Yugang Yu is a Professor of Logistics and Operations Management at the University of Science and Technology of China, PR China (USTC). He obtained his Ph.D. in Management Science and Engineering from the School of Management, USTC, in 2003. His current research interests are in warehousing, supply chain management, and data-driven research in OM and application of Operations Research. He has published more than 60 papers in academic journals, including *Productions and Operations Management*, *Transportation Science*, *IISE Transactions*, *International Journal of Production Research*, *European Journal of Operational Research*, *Annals of Operations Research*, *IEEE Transactions on Automation Science and Engineering*, *and International Journal of Production Economics*. His papers have been cited more than 1500 times, and he is among the most cited researchers in China. His research results have also led to several patents in China. He has received a career development project award from The Netherlands Organization for Scientific Research, a distinguished research scholar grant from the National Science Foundation of China, and Yangtze Scholar Distinguished Professorship from the China Ministry of Education.

René B. M. de Koster is a Professor of Logistics and Operations Management at the Rotterdam School of Management, Erasmus University. His research interests are warehousing, terminal, and behavioral operations. He is the author/editor of eight books and over 150 papers in books and journals. He has been a guest lecturer at universities in Belgium, China, and South Africa. He is/was on the editorial boards of *Operations Research*, *Journal of Operations Management*, *Transportation Science* (SI editor), and other journals. He is member of several international research advisory boards (such as European Logistics Association and BVL, www.bvl.de). He is the chairman of Stichting Logistica and founder of the Material Handling Forum (www.rsm.nl/mhf). His research has received several awards (*IIE Transactions* 2009, 2016; *Journal of Operations Management* finalist 2007; *Academy of Management* best paper finalist 2013).

References

Bozer, Y.A. and White, J.A. (1984) Travel-time models for automated storage/retrieval systems. *IIE Transactions*, **16**(4), 329–338.

De Koster, M.B.M., Le-Duc, T. and Yu, Y. (2008) Optimal storage rack design for a 3-dimensional compact AS/RS. *International Journal of Production Research*, **46**(6), 1495–1514.

Eynan, A. and Rosenblatt, M.J. (1994) Establishing zones in single-command class-based rectangular AS/RS. *IIE Transactions*, **26**(1), 38–46.

Fukunari, M. and Malmborg, C.J. (2007) An efficient cycle time model for autonomous vehicle storage and retrieval systems. *International Journal of Production Research*, **46**(12), 3167–3184.

Graves, S.C., Hausman, W.H. and Schwarz, L.B. (1977) Storage-retrieval interleaving in automatic warehousing systems. *Management Science*, **23**(9), 935–945.

Gue, K.R. and Kim, B.S. (2007) Puzzle-based storage systems. *Naval Research Logistics*, **54**(5), 556–567.

Han, M.H., McGinnis, L.F., Shieh, J.S. and White, J.A. (1987) On sequencing retrievals in an automated storage/retrieval system. *IIE Transactions*, **19**(1), 56–66.

Hausman, W.H., Schwarz, L.B. and Graves, S.C. (1976) Optimal storage assignment in automatic warehousing systems. *Management Science*, **22**(6), 629–638.

Hyundai Elevator. (2012) Hyundai integrated parking system (HIP). Available at http://hyundaielevator.co.kr/eng/parking/car/automobile.jsp. [29 November 2016].

Johnson, M.E. and Brandeau, M.L. (1996) Stochastic modeling for automated material handling system design and control. *Transportation Science*, **30**(4), 330–350.

Keserla, A. and Peters, B.A. (1994) Analysis of dual-shuttle automated storage/retrieval systems. *Journal of Manufacturing Systems*, **13**(6), 424–434.

Kim, J. and Seidmann, A. (1990) A framework for the exact evaluation of expected cycle times in automated storage systems with full-turnover item allocation and random service requests. *Computers and Industrial Engineering*, **18**(4), 601–612.

Kouvelis, P. and Papanicolaou, V. (1995) Expected travel-time and optimal boundary formulas for a 2-class-based automated storage-retrieval system. *International Journal of Production Research*, **33**(10), 2889–2905.

Kuo, P.H., Krishnamurthy, A. and Malmborg, C.J. (2007) Design models for unit load storage and retrieval systems using autonomous vehicle technology and resource conserving storage and dwell point policies. *Applied Mathematical Modeling*, **31**, 2332–2346.

Magic Black Box. (2012) Available at http://www.odth.be/magic-black-box. [29 November 2016].

Malmborg, C.J. (2000) Interleaving models for the analysis of twin shuttle automated storage and retrieval systems. *International Journal of Production Research*, **38**(18), 4599–4610.

Malmborg, C.J. (2002) Conceptualizing tools for autonomous vehicle storage and retrieval systems. *International Journal of Production Research*, **40**(8), 1807–1822.

Mirzaei, M., de Koster, R.B.M. and Zaerpour, N. (2017) Modelling load retrievals in puzzle-based storage systems. *International Journal of Production Research*, Working paper.

Park, B.C. (2006) Performance of automated storage/retrieval systems with non-square-in-time racks and two-class storage. *International Journal of Production Research*, **44**(6), 1107–1123.

Park, B.C., Foley, R.D., White, J.A. and Frazelle, E.H. (2003) Dual command travel times and miniload system throughput with turnover-based storage. *IIE Transactions*, **35**(4), 343–355.

Park, Swipe, Leave Systems. (2012) Available at http://www.automotionparking.com/index.php. [29 November 2016].

Roodbergen, K.J. and Vis, I.F.A. (2009) A survey of literature on automated storage and retrieval systems. *European Journal of Operational Research*, **194**(2), 343–362.

Rosenblatt, M.J. and Eynan, A. (1989) Deriving the optimal boundaries for class-based automatic storage/retrieval systems. *Management Science*, **35**(12), 1519–1524.

Roy, D., Krishnamurthy, A., Heragu, S. and Malmborg, C. (2015) Queuing models to analyze dwell-point and cross-aisle location in autonomous vehicle-based warehouse systems. *European Journal of Operational Research*, **242**(1), 72–87.

Ruben, R.A. and Jacobs, F.R. (1999) Batch construction heuristics and storage assignment strategies for walk/ride and pick systems. *Management Science*, **45**(4), 575–596.

Sarker, B.R., Sabapathy, A., Lal, A.M. and Han, M.H. (1991) Performance evaluation of a double shuttle automated storage and retrieval system. *Production Planning and Control*, **2**(3), 207–213.

Sari, Z., Saygin, C., Ghouali, N. (2005) Travel-time models for flowrack automated storage and retrieval systems. *International Journal of Advanced Manufacturing Technology*, **25**, 979–987.

Slocum, J., and Sonneveld, D. (2006) *The 15 Puzzle Book*, Slocum Puzzle Foundation, Beverly Hills, CA.

Space Parking Optimization Technology. (2012) Available at http://www.youtube.com/watch?v=eu7pRjI6APM. [29 November 2016].

Stadtler, H. (1996) An operational planning concept for deep lane storage systems. *Production and Operations Management*, **5**, 266–282.

UCW Container Storage System. (2012) Available at http://www.ezindus.com. [29 November 2016].

Wohr Parksafe. (2012) Available at http://www.woehr.de/en/project/liverpool-parksafe-583.html. [29 November 2016].

Yu, Y. and de Koster, M.B.M. (2009) Optimal zone boundaries for two-class-based compact three-dimensional automated storage and retrieval systems. *IIE Transactions*, **41**(3), 194–208.

Yu, Y. and de Koster, M.B.M. (2012) Sequencing heuristics for storing and retrieving unit loads in 3D compact automated warehousing systems. *IIE Transactions*, **44**(2), 69–87.

Zaerpour, N., Yu, Y. and de Koster, R.B.M. (2015) Storing fresh produce for fast retrieval in an automated compact cross-dock system. *Production and Operations Management*, **24**(8), 1266–1284.

Zaerpour, N., Yu, Y., and de Koster, R.B.M. (2017) Small is beautiful: A framework for evaluating and optimizing live-cube compact storage systems. *Transportation Science*, **51**(1), 34–51; http://dx.doi.org/10.1287/trsc.2015.0586.

Zaerpour, N., Yu, Y., and de Koster, R.B.M. (2017) Supplement for response time analysis of a two-class based live-cube compact storage system. (Working paper), Rotterdam School of Management, Erasmus University.

Appendices

Appendix A: V^1, $E[T^1]$, and $E[T^2]$ for all sub-cases

We give closed-form formulas of the volume of the first zone (V^1), $E[T^1]$, and $E[T^2]$ for all sub-cases A1 , . . . , P3 In Tables A1 to A3.

Table A1. Volume formulas for first zones of sub-cases A1 , . . . , P3.

Sub-case	Volume formula (V^1)
A1, A2, A3, A4	$\dfrac{7b^3}{48}$
B1, B2, B3, B4	$\dfrac{1}{48}(-b^3 + 24b(b-w)w + 8w^3)$
C1, C2, C3, C4	$\dfrac{1}{48}(-b^3 - 8(b-l)^3 + 24b(b-w)w + 8w^3)$
D2, D3, D4	$\dfrac{1}{8}b(3b - 2w)w$
E2, E3, E4	$-\dfrac{1}{6}(b-l)^3 + \dfrac{1}{8}b(3b-2w)w$
F2, F3, F4	$-\dfrac{1}{24}w(3b^2 - 6b(4l+w) + 4(3l^2 + 3lw + w^2))$
G3, G4	$\dfrac{1}{48}(24blw + (b - 2(l+w))^3)$
H4	$\dfrac{blw}{2}$
I1	$\dfrac{1}{6}h(3b^2 - 3bh + h^2)$
J1	$\dfrac{1}{6}(-b^3 + h^3 + w^3 + 3b^2(h+w) - 3b(h^2+w^2))$
K1	$\dfrac{1}{6}(-2b^3 + h^3 + l^3 + w^3 + 3b^2(h+l+w) - 3b(h^2+l^2+w^2))$
L1, L2	$-\dfrac{1}{2}hw(-2b + h + w)$
M1, M2	$-\dfrac{1}{6}(b-l)^3 - \dfrac{1}{2}hw(-2b + h + w)$
N2	$-\dfrac{1}{6}w(3b^2 + 3h^2 + 3l^2 + 3hw + 3lw + w^2 - 3b(2h + 2l + w))$
O1	$\dfrac{1}{6}(6hlw + (-b + l + w)^3 - (-b + h + l + w)^3)$
P1, P2, P3	$hlw - \dfrac{1}{6}(-b + h + l + w)^3$

Table A2. $E[T^1]$ of all sub-cases.

Sub-case	$E[T^1]$ closed-form formula
A1, A2, A3, A4	$\dfrac{3b}{4}$
B1, B2, B3, B4	$\dfrac{3b^4 - 64b^3w + 48b^2w^2 - 8w^4}{4b^3 - 96b^2w + 96bw^2 - 32w^3}$
C1, C2, C3, C4	$\dfrac{27b^4 - 64b^3(l+w) + 48b^2(l^2+w^2) - 8(l^4+w^4)}{4(9b^3 - 24b^2(l+w) + 24b(l^2+w^2) - 8(l^3+w^3))}$
D2, D3, D4	$-\dfrac{-6b^3 + 3b^2w + w^3}{9b^2 - 6bw}$
E2, E3, E4	$\dfrac{3b^4 - l^4 + w^4 - 2b^3(4l+3w) + 3b^2(2l^2+w^2)}{4b^3 - 4l^3 - 3b^2(4l+3w) + 6b(2l^2+w^2)}$
F2, F3, F4	$\dfrac{2b^3 - 3b^2(4l+w) + 2(2l^3 + 3l^2w + 2lw^2 + w^3)}{3b^2 - 6b(4l+w) + 4(3l^2 + 3lw + w^2)}$
G3, G4	$\dfrac{3b^4 - 16b^3(l+w) - 16(l^2+lw+w^2)^2 + 24b^2(l^2+4lw+w^2)}{4(b^3 - 6b^2(l+w) - 8(l+w)^3 + 12b(l^2+4lw+w^2))}$
H4	$\dfrac{3b^2 + 2l^2 + 3lw + 2w^2}{6b}$
I1	$\dfrac{4b^3 - 3b^2h + h^3}{6b^2 - 6bh + 2h^2}$
J1	$-\dfrac{-3b^4 + 2h^4 + w^4 + 8b^3(h+w) - 6b^2(h^2+w^2)}{4(b^3 - h^3 - w^3 - 3b^2(h+w) + 3b(h^2+w^2))}$
K1	$-\dfrac{6b^4 - 2h^4 - l^4 - w^4 - 8b^3(h+l+w) + 6b^2(h^2+l^2+w^2)}{4(-2b^3 + h^3 + l^3 + w^3 + 3b^2(h+l+w) - 3b(h^2+l^2+w^2))}$
L1	$\dfrac{-h^3 + 4h^2w + 6hw^2 + 4w(-3b^2+w^2)}{12w(-2b+h+w)}$
L2	$\dfrac{-12b^2h + 12h^2w + w^3}{12h(-2b+h+w)}$
M1	$-\dfrac{-3b^4 + h^4 + 8b^3l + l^4 - 4h^3w - 6h^2w^2 - 4hw^3 - 6b^2(l^2 - 2hw)}{4(b^3 - 3b^2l - l^3 + 3hw(h+w) + 3b(l^2 - 2hw))}$
M2	$\dfrac{3b^4 - 8b^3l - l^4 + 12h^2w^2 + w^4 + 6b^2(l^2 - 2hw)}{4(b^3 - 3b^2l - l^3 + 3hw(h+w) + 3b(l^2 - 2hw))}$
N2	$\dfrac{4b^3 + 2l^3 + 6h^2w + 3l^2w + 2lw^2 + w^3 - 3b^2(2h+2l+w)}{2(3b^2 + 3h^2 + 3l^2 + 3hw + 3lw + w^2 - 3b(2h+2l+w))}$
O1	$\dfrac{4b^3 + 2h^2(l+w) + 3h(l^2+w^2) + 2(l^3+w^3) - 3b^2(h+2(l+w))}{2(3b^2 + h^2 + 3h(l+w) + 3(l^2+w^2) - 3b(h+2(l+w)))}$
P1	$-\dfrac{3b^4 - 4h^3(l+w) - (l+w)^4 - 8b^3(h+l+w) + 6b^2(h+l+w)^2 - 6h^2(l^2+w^2) - 4h(l^3+w^3)}{4(-b^3 + h^3 + 3h^2(l+w) + (l+w)^3 + 3b^2(h+l+w) - 3b(h+l+w)^2 + 3h(l^2+w^2))}$
P2	$-\dfrac{3b^4 - h^4 - 4h^3l - 6h^2l^2 - 4hl^3 - l^4 - 4l^3w - 12h^2w^2 - 6l^2w^2 - 4lw^3 - 2w^4 - 8b^3(h+l+w) + 6b^2(h+l+w)^2}{4(-b^3 + h^3 + 3h^2(l+w) + (l+w)^3 + 3b^2(h+l+w) - 3b(h+l+w)^2 + 3h(l^2+w^2))}$
P3	$-\dfrac{3b^4 - 8b^3(h+l+w) + 6b^2(h+l+w)^2 - 2(h^4 + 6h^2(l^2+w^2) + (l^2+lw+w^2)^2)}{4(-b^3 + h^3 + 3h^2(l+w) + (l+w)^3 + 3b^2(h+l+w) - 3b(h+l+w)^2 + 3h(l^2+w^2))}$

Table A3. $E[T^2]$ of all sub-cases.

Sub-case	$E[T^2]$ closed-form formula
A1	$\dfrac{21b^4 - 8h(h^3 + 12hlw + 12lw(l + w))}{4(7b^3 - 48hlw)}$
A2	$\dfrac{21b^4 - 8w(4h^3 + 6h^2(2l - w) - w^3 + 4h(3l^2 + 3lw + w^2))}{4(7b^3 - 48hlw)}$
A3	$\dfrac{21b^4 + 8(h^4 + l^4 + 6h^2(l - w)^2 + w^4 - 4h^3(l + w) - 4h(l + w)^3)}{4(7b^3 - 48hlw)}$
A4	$\dfrac{21b^4 - 16lw(12h^2 + 2l^2 + 3lw + 2w^2)}{4(7b^3 - 48hlw)}$
B1	$\dfrac{3b^4 - 64b^3w + 48b^2w^2 + 8(h^4 + 12h^2lw - w^4 + 12hlw(l + w))}{4(b^3 - 24b^2w + 48hlw + 24bw^2 - 8w^3)}$
B2	$\dfrac{3b^4 - 64b^3w + 48b^2w^2 + 16w(2h^3 + h^2(6l - 3w) - w^3 + 2h(3l^2 + 3lw + w^2))}{4(b^3 - 24b^2w + 48hlw + 24bw^2 - 8w^3)}$
B3	$\dfrac{3b^4 - 64b^3w + 48b^2w^2 - 8(h^4 + l^4 + 6h^2(l - w)^2 + 2w^4 - 4h^3(l + w) - 4h(l + w)^3)}{4(b^3 - 24b^2w + 48hlw + 24bw^2 - 8w^3)}$
B4	$\dfrac{3b^4 - 64b^3w + 48b^2w^2 + 8w(24h^2l + 4l^3 + 6l^2w + 4lw^2 - w^3)}{4(b^3 - 24b^2w + 48hlw + 24bw^2 - 8w^3)}$
C1	$\dfrac{27b^4 - 64b^3(l + w) + 48b^2(l^2 + w^2) + 8(h^4 - l^4 + 12h^2lw - w^4 + 12hlw(l + w))}{4(9b^3 - 24b^2(l + w) + 24b(l^2 + w^2) - 8(l^3 - 6hlw + w^3))}$
C2	$\dfrac{27b^4 - 64b^3(l + w) + 48b^2(l^2 + w^2) + 8(-l^4 + 12hl^2w + 12hlw(h + w) - 2w(-2h^3 + 3h^2w - 2hw^2 + w^3))}{4(9b^3 - 24b^2(l + w) + 24b(l^2 + w^2) - 8(l^3 - 6hlw + w^3))}$
C3	$\dfrac{27b^4 - 64b^3(l + w) + 48b^2(l^2 + w^2) - 8(h^4 + 6h^2(l - w)^2 - 4h^3(l + w) - 4h(l + w)^3 + 2(l^4 + w^4))}{4(9b^3 - 24b^2(l + w) + 24b(l^2 + w^2) - 8(l^3 - 6hlw + w^3))}$
C4	$\dfrac{27b^4 - 64b^3(l + w) + 48b^2(l^2 + w^2) - 8(l^4 - 4l^3w - 6l^2w^2 + w^4 - 4l(6h^2w + w^3))}{4(9b^3 - 24b^2(l + w) + 24b(l^2 + w^2) - 8(l^3 - 6hlw + w^3))}$
D2	$\dfrac{6b^3 - 3b^2w - 2h(2h^2 + 6hl + 6l^2 - 3hw + 6lw + 2w^2)}{9b^2 - 24hl - 6bw}$
D3	$-\dfrac{h^4 + l^4 + 6h^2(l - w)^2 + 3b^2(2b - w)w - 4h^3(l + w) - 4h(l + w)^3}{3w(-3b^2 + 8hl + 2bw)}$
D4	$-\dfrac{-6b^3 + 24h^2l + 4l^3 + 3b^2w + 6l^2w + 4lw^2 + w^3}{3(3b^2 - 8hl - 2bw)}$
E2	$\dfrac{3b^4 - l^4 + 12hl^2w + 12hlw(h + w) - 2b^3(4l + 3w) + 3b^2(2l^2 + w^2) + 2hw(2h^2 - 3hw + 2w^2)}{4b^3 - 3b^2(4l + 3w) - 4l(l^2 - 6hw) + 6b(2l^2 + w^2)}$
E3	$\dfrac{3b^4 - h^4 - 2l^4 - 6h^2(l - w)^2 + 4h^3(l + w) + 4h(l + w)^3 - 2b^3(4l + 3w) + 3b^2(2l^2 + w^2)}{4b^3 - 3b^2(4l + 3w) - 4l(l^2 - 6hw) + 6b(2l^2 + w^2)}$
E4	$\dfrac{3b^4 - l^4 + 4l^3w + 6l^2w^2 + w^4 - 2b^3(4l + 3w) + 3b^2(2l^2 + w^2) + 4l(6h^2w + w^3)}{4b^3 - 3b^2(4l + 3w) - 4l(l^2 - 6hw) + 6b(2l^2 + w^2)}$
F2	$\dfrac{2b^3 + 4h^3 + 4l^3 + 6h^2(2l - w) + 6l^2w + 4lw^2 + w^3 - 3b^2(4l + w) + 4h(3l^2 + 3lw + w^2)}{3b^2 - 6b(4l + w) + 4(6hl + 3l^2 + 3lw + w^2)}$
F3	$\dfrac{-h^4 - l^4 - 6h^2(l - w)^2 + 4l^3w + 6l^2w^2 + (b - w)^2w(2b + w) + 4h^3(l + w) + 4h(l + w)^3 + 4lw(-3b^2 + w^2)}{w(3b^2 - 6b(4l + w) + 4(6hl + 3l^2 + 3lw + w^2))}$
F4	$\dfrac{2b^3 - 3b^2(4l + w) + 2(12h^2l + 4l^3 + 6l^2w + 4lw^2 + w^3)}{3b^2 - 6b(4l + w) + 4(6hl + 3l^2 + 3lw + w^2)}$
G3	$\dfrac{3b^4 - 16b^3(l + w) + 24b^2(l^2 + 4lw + w^2) + 8(h^4 + 6h^2(l - w)^2 - 4h^3(l + w) - 4h(l + w)^3 - (l + w)^4)}{4(b^3 - 6b^2(l + w) + 12b(l^2 + 4lw + w^2) - 8(l^3 + 3l^2w + w^3 + 3lw(2h + w)))}$
G4	$\dfrac{-3b^4 + 16b^3(l + w) - 24b^2(l^2 + 4lw + w^2) + 16(l^4 + 4l^3w + 6l^2w^2 + w^4 + 4l(3h^2w + w^3))}{32\left(-3blw + 6hlw + \left(-\dfrac{b}{2} + l + w\right)^3\right)}$

(Continued on next page)

Table A3. $E[T^2]$ of all sub-cases. (*Continued*)

Sub-case	$E[T^2]$ closed-form formula
H4	$\dfrac{b}{2} + h$
I1	$\dfrac{8b^3 - 6b^2h + h^3 - 12hlw - 12lw(l+w)}{4(3b^2 - 3bh + h^2 - 6lw)}$
J1	$-\dfrac{-3b^4 + h^4 - 12h^2lw + w^4 + 8b^3(h+w) - 12hlw(l+w) - 6b^2(h^2+w^2)}{4(b^3 - h^3 + 6hlw - w^3 - 3b^2(h+w) + 3b(h^2+w^2))}$
K1	$-\dfrac{6b^4 - h^4 - l^4 + 12h^2lw - w^4 + 12hlw(l+w) - 8b^3(h+l+w) + 6b^2(h^2+l^2+w^2)}{4(-2b^3 + h^3 + l^3 - 6hlw + w^3 + 3b^2(h+l+w) - 3b(h^2+l^2+w^2))}$
L1, L2	$-\dfrac{6b^2 - 2h^2 - 6hl - 6l^2 - 3hw - 6lw - 2w^2}{6(-2b+h+2l+w)}$
M1, M2	$\dfrac{3b^4 - 8b^3l - l^4 + 12hl^2w + 12hlw(h+w) + 6b^2(l^2 - 2hw) + 2hw(2h^2 + 3hw + 2w^2)}{4(b^3 - 3b^2l - l^3 + 6hlw + 3hw(h+w) + 3b(l^2 - 2hw))}$
N2	$\dfrac{w^2(4(h+l)+w)}{4(3(-b+h+l)^2 + 3(-b+h+l)w + w^2)} + \dfrac{4b^3 - 3b^2(2(h+l)+w) + (h+l)^2(2(h+l)+3w)}{6(-b+h+l)^2 + 6(-b+h+l)w + 2w^2}$
O1	$\dfrac{8b^3 + h^3 + 4h^2(l+w) + 6h(l+w)^2 + 4(l+w)^3 - 6b^2(h+2(l+w))}{4(3b^2 + h^2 + 3h(l+w) + 3(l+w)^2 - 3b(h+2(l+w)))}$
P1, P2, P3	$\dfrac{1}{4}(3b + h + l + w)$

Table A4. $E[T^1]$ and $E[T^2]$ for two-class-based storage with a cuboid first zone.

Case	$E[T]$ formula
A ($h \leq w$)	$E[T_A^1] = \dfrac{G^{1/3}(12l^2w + h^3 + 12lw(w+h))}{24lw}$
	$E[T_A^2] = \dfrac{(-1+G^{4/3})(h^3 + 12hlw + 12lw(l+w))}{24(-1+G)lw}$
B ($w \leq h \leq l$)	$E[T_B^1] = \dfrac{G^{1/3}(-w^3 + 4w^2h + 6w(2l-h)h + 4h(3l^2 + 3lh + h^2))}{24lh}$
	$E[T_B^2] = \dfrac{(-1+G^{4/3})(4h^3 + 6h^2(2l-w) - w^3 + 4h(3l^2 + 3lw + w^2))}{24(-1+G)hl}$
C ($l \leq h \leq l+w$)	$E[T_C^1] = -\dfrac{G^{1/3}(l^4 + (w-h)^4 - 4l^3h + 6l^2h(-2w+h) - 4lh(3w^2 + 3wh + h^2))}{24lwh}$
	$E[T_C^2] = -\dfrac{(-1+G^{4/3})(h^4 + l^4 + 6h^2(l-w)^2 + w^4 - 4h^3(l+w) - 4h(l+w)^3)}{24(-1+G)hlw}$
D ($l+w \leq h$)	$E[T_D^1] = \dfrac{G^{1/3}(2l^2 + 3lw + 2(w^2 + 6h^2))}{12h}$
	$E[T_D^2] = \dfrac{(1 + G^{1/3} + G^{2/3} + G)(12h^2 + 2l^2 + 3lw + 2w^2)}{12(1 + G^{1/3} + G^{2/3})h}$

Appendix B: Derivation of $E[T^1]$ and $E[T^2]$ for a two-class-based live-cube system with a cuboid first zone

Figure A1 illustrates a two class-based live-cube system with a cuboid first zone. $E[T^1]$ can simply be calculated by using the results of Zaerpour *et al.* (2017). It only suffices to use the closed-form formulas obtained for random storage and replace l_1, w_1, and h_1 by $G^{1/3}l$, $G^{1/3}w$, $G^{1/3}h$, respectively, where l_1, w_1, and h_1 are the dimensions of the first zone, l, w, h are the dimensions of the live-cube system, and G is the relative size of the first zone.
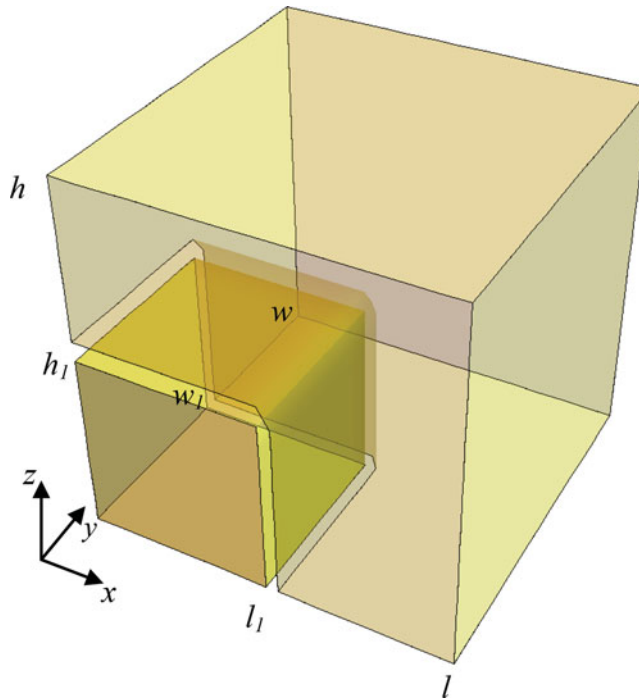

Figure A1. A two-class-based live-cube system with a cuboid first zone.

We know that $E[T]$ of a live-cube system under random storage equals the weighted average of any two storage zones. Thus, we have $E[T] = G\,E[T^1] + (1 - G)\,E[T^2]$. Consequently, $E[T^2]$ can be calculated as follows, $E[T^2] = (E[T] - G\,E[T^1])/(1 - G)$. Since Zaerpour *et al.* (2017) obtain four closed-form formulas corresponding to four different cases, $E[T^1]$ and $E[T^2]$ are also obtained for these four cases (see Table A4). $E[T]$ of the two-class-based storage with a cuboid first zone can then be calculated using Equation (4).